Algal Research 6 (2014) 250–270

Contents lists available at ScienceDirect

Algal Research

journal homepage: www.elsevier.com/locate/algal

Getting to low-cost algal biofuels: A monograph on conventional and cutting-edge harvesting and extraction technologies

James E. Coons *, Daniel M. Kalb, Taraka Dale, Babetta L. Marrone

Chemistry and Bioscience Divisions, Los Alamos National Laboratory, Los Alamos, NM 87545, USA

ARTICLE INFO

Article history:
Received 2 December 2013
Received in revised form 31 July 2014
Accepted 7 August 2014
Available online 31 August 2014

Keywords:
Harvesting
Extraction
Membrane filtration
Electrocoagulation
Centrifugation
Ultrasound

ABSTRACT

Among the most formidable challenges to algal biofuels is the ability to harvest algae and extract intracellular lipids at low cost and with a positive energy balance. In this monograph, we construct two paradigms that contrast energy requirements and costs of conventional and cutting-edge Harvesting and Extraction (H&E) technologies. By application of the parity criterion and the moderate condition reference state, an energy–cost paradigm is created that allows 1st stage harvesting technologies to be compared with easy reference to the National Alliance for Advanced Biofuels and Bioproducts (NAABB) target of $0.013/gallon of gasoline equivalent (GGE) and to the U.S. DOE's Bioenergy Technologies Office 2022 cost metrics. Drawing from the moderate condition reference state, a concentration-dependency paradigm is developed for extraction technologies, making easier comparison to the National Algal Biofuels Technology Roadmap (NABTR) target of less than 10% total energy. This monograph identifies cost-bearing factors for a variety of H&E technologies, describes a design basis for ultrasonic harvesters, and provides a framework to measure future technological advancements toward reducing H&E costs. Lastly, we show that ultrasonic harvesters and extractors are uniquely capable of meeting both NAABB and NABTR targets. Ultrasonic technologies require further development and scale-up before they can achieve low-cost performance at industrially relevant scales. However, the advancement of this technology would greatly reduce H&E costs and accelerate the commercial viability of algae-based biofuels.

1. Introduction

Interest in microalgae as an alternative source of transportation fuel grew from the oil embargo of 1973 to become a significant component of today's energy policy [1,2]. While events described below denote governmental action in the U.S., renewable fuels are clearly of global interest and have come to be mandated in many countries [3]. In 1978, the Aquatic Species Program (ASP) was created and soon focused on the development of microalgae as a renewable source of diesel [1]. Over its 18-year lifetime, the ASP revealed that large-scale production of algal biofuel would not threaten water or land resources, that as much as 20% of crude oil consumed could be replaced by microalgae grown with waste CO_2 from power plants, and that the main barrier to algal biofuels is their high cost. A renewed interest in algal biofuels ensued with the climb in crude oil prices that began in the early 2000's. The Renewable Fuel Standard (RFS), initially established in 2005 and expanded in 2007, mandates the inclusion of at least 36 billion gallons of renewable biofuel by the year 2022 [4]. In late 2008, the National Algal Biofuels Technology Roadmap (NABTR) Workshop was convened to identify critical challenges hindering the economical production of algal biofuels at commercial scale. Among the barriers considered, conventional Harvesting & Extraction (H&E) processes were determined to be costly, energy intensive, and in need of innovation. The term "extraction" was applied more generally in the NABTR report to include various technologies positioned between harvesting and conversion in the biofuels production process. In early 2009, the National Alliance for Advanced Biofuels and Bioproducts (NAABB) consortium was created to produce new technologies toward achieving a viable algal biofuel industry. NAABB set a challenging target: Identify and develop technologies capable of harvesting algae at less than $0.013/GGE at a processing rate of 0.1 to 1 m^3 of algal water per hour, which is roughly an order of magnitude less costly than targets from the late 1970's [5]. NABTR included the following benchmark for extraction: Consume no more than 10% of the total energy available from the produced algae. Marginalizing the costs of H&E would position algal biofuels more competitively, but cost reductions in all areas will be needed to meet the 2022 cost metrics set by the U.S. Department of Energy's Bioenergy Technologies Office (BETO) [2]. Here two novel paradigms are described to compare H&E technologies and identify those capable of meeting the NAABB and NABTR targets. Although these targets were created with a U.S. market in mind, meeting them also assures the sustainability of H&E processes. Sustainability is achieved when production energy is less than the energy

* Corresponding author at: MS J964, Chemistry Division, Los Alamos National Laboratory, Los Alamos, NM 87545, USA. Tel.: +1 505 667 6362.
E-mail address: jimc@lanl.gov (J.E. Coons).

http://dx.doi.org/10.1016/j.algal.2014.08.005

Nomenclature

$A_{Harvester}$ is the area normal to the direction of flow in a harvester, m^2.
ASP is the Aquatic Species Program.
$[B]$ is the mass of algae per unit volume of algal water, kg (dry mass) of algae/m^3.
$[B]_{Extraction}$ is the mass of algae per unit volume of algal water at the time of extraction, kg (dry mass) of algae/m^3.
$[B]_{Harvesting}$ is the mass of algae per unit volume of algal water at the time of harvest, kg (dry mass) of algae/m^3.
BETO is the Bioenergy Technologies Office, which is one of eleven technology development offices within the U.S. Department of Energy's Office of Energy Efficiency & Renewable Energy.
Btu is British thermal unit.
$\overline{C}$ is the cost per unit volume of algal water, \$/m^3.
C_{Lipid}^* is the cost contribution to the price of algal lipid, \$/GGE.
$C_{Electricity}^*$ is the cost of electricity, \$/kWh.
$\overline{C}_{Electrolytic}$ is the cost per unit volume of algal water needed for electrolytic processes, \$/m^3.
$\overline{C}_{Membrane,\ High}$ is the upper estimate of O&M costs of cross flow membrane filtration per unit volume of algal water, \$/m^3.
$\overline{C}_{Membrane,\ Low}$ is the lower estimate of O&M costs of cross flow membrane filtration per unit volume of algal water, \$/m^3.
C_{Metal} is the cost of the electrode metal, \$/kg.
$\widetilde{C}_P^*$ is the heat capacity of a liquid at constant pressure, kWh/(kg°C).
c_{Algae} is the speed of sound through an algae cell, m/s.
c_{Media} is the speed of sound through the media, m/s.
CEPCI is the Chemical Engineering Plant Cost Index.
$\dot{D}_{Metal}^*$ is the anode metal dissolution rate, kg/(ampere hour).
D_{Pipe} is the internal pipe diameter, m.
d_{Algae} is the diameter of the algae cells, m.
DME is dimethyl ether.
$\overline{E}$ is the energy input per unit volume of algal water, J/m^3.
$\overline{E}^*$ is the energy input per unit volume of algal water, kWh/m^3.
$\overline{E}_{Centrifuge}$ is the energy required for centrifugation per unit volume of algal water, J/m^3.
$\overline{E}_{Centrifuge}^*$ is the energy required for centrifugation per unit volume of algal water, kWh/m^3.
$\overline{E}_{Disk}^*$ is the energy required for a disk centrifugation per unit volume of algal water, kWh/m^3.
$\overline{E}_{Extraction}^*$ is the energy required for extraction per unit volume of algal water, kWh/m^3.
$\hat{E}_{Extraction}^*$ is the specific energy required for extraction, kWh/kg (dry mass) of algae.
$\overline{E}_{Lipid}^*$ is the energy content of the lipid per unit volume of algal water, kWh/m^3.
$\overline{E}_{Lipid}^{Available,*}$ is the energy content of the available lipid per unit volume of algal water, kWh/m^3.
$\overline{E}_{LEA}^*$ is the energy in the Lipid Extracted Algae (LEA) per unit volume of algal water, kWh/m^3.
$\overline{E}_{Pump}$ is the energy required for pumping per unit volume of algal water, J/m^3.
$\overline{E}_{Pump}^*$ is the energy required for pumping per unit volume of algal water, kWh/m^3.
$\langle \overline{E}_S \rangle$ is the time-averaged energy density of the standing wave in the algal water, J/m^3.
$\overline{E}_{Total}^*$ is the total energy from both lipid and LEA per unit volume of algal water, kWh/m^3.
$\widetilde{E}_{Total}^*$ is the total energy from both lipid and LEA per kg of media, kWh/kg.
$\hat{E}_{Total}^*$ is the total energy from both lipid and LEA per dry mass of algae, kWh/kg (dry weight) of algae.
$\overline{E}_{Tubular\ \&\ Helical}^*$ is the energy required for a tubular or helical centrifuge per unit volume of algal water, kWh/m^3.
$\overline{E}_{Ultrasonic}$ is the (input) energy required for an ultrasonic harvester per unit volume of algal water, J/m^3.
$\overline{E}_{Ultrasonic}^*$ is the (input) energy required for an ultrasonic harvester per unit volume of algal water, kWh/m^3.
$\widetilde{E}_{Vaporization}^*$ is the energy required to vaporize a unit mass of liquid, kWh/kg.
EEF is the Energy Efficiency Factor, s^{-1}.
EPA is the Environmental Protection Agency.
F_{Drag} is the drag force experienced by a particle moving through a viscous media, N.
F_{Drying} is the fraction of total energy consumed by drying, dimensionless.
F_{Energy} is the fraction of total energy consumed for extraction, dimensionless.
$F_{Gravity}$ is the force experienced by a particle due to gravity, N.
F_S is the ultrasonic radiation force exerted on a particle in a standing wave, N.
$F_{Sensible}$ is the fraction of total energy consumed by sensible heating, dimensionless.
f is the cyclical frequency, Hz.
$f_{Friction}$ is the friction factor used with the Fanning equation, dimensionless.
g_c is the gravitational constant, 9.8 m/s^2.
GGE is gallon of gasoline equivalent, U.S. gallons.
ΔH_{LEA}^* is the heat of combustion of the Lipid Extracted Algae per unit mass, kWh/kg.
ΔH_{Lipid}^* is the heat of combustion of the lipid per unit mass, kWh/kg lipid.
H&E is Harvesting and Extraction.
HHV^* is the higher heating value, Btu/gal.
HHV is the higher heating value.
HPH is High Pressure Homogenization.
I is the electrical current, ampere.
$\hat{I}^*$ is the specific charge of the algae [see Eq. (21)], ampere hour/kg (dry weight) algae.
K_S is the acoustic contrast of the algae, dimensionless.
L_e is the equivalent length of piping due to frictional losses, m.
$[L]_{Harvesting}$ is the mass of lipid per unit volume of algal water at the time of harvest, kg/m^3.
$[L]_{Harvesting}^{Available}$ is the available mass of lipid per unit volume of algal water at the time of harvest, kg/m^3.
$L_{Horizontal}$ is the horizontal length of piping, m.
L_{UF} is the length of the ultrasonic field in the direction of flow, m.
$L_{Vertical}$ is the vertical length of piping, m.
LEA is Lipid Extracted Algae.
$\hat{M}_{Lipid}$ is the mass ratio of lipid to algae mass (dry weight), kg of lipid/kg of algae (dry weight).
$\hat{M}_{Solvent}$ is the mass ratio of solvent to algae, kg of solvent/kg (dry weight) of algae.
$\widetilde{M}_{Solvent}$ is the mass ratio of solvent to media, kg of solvent/kg of media.
N_{Re} is the Reynolds number, dimensionless.
n is an integer number, dimensionless.
NAABB is the National Alliance for Advanced Biofuels and Bioproducts.
NABTR is the National Algal Biofuels Technology Roadmap.
O&M is Operating and Maintenance.
P is power, W.

$\overline{P}_{Algae}$ is a number dependent on algae properties as defined by Eq.(40), W/m^3.
P_{App} is the apparent power input to the acoustic harvester, W.
$\overline{P}_{App}$ is the apparent power density input to the acoustic harvester, W/m^3.
P_{Pump} is the power required for pumping algal water to the overhead feed tank, W.
Q is flow rate, m^3/s.
Q^* is flow rate (or permeate rate for cross flow filtration), m^3/h.
Q_{Actual}^* is the actual feed (flow) rate to the centrifuge, m^3/h.
Q_{Feed} is the feed (flow) rate of algal water, generally in units of m^3/s.
Q_{Master}^* is the centrifuge flow rate taken from the master curve, m^3/h.
r is the radius of the centrifuge, m.
RD is renewable diesel.
RFS is the Renewable Fuel Standard.
SPR is the Strategic Petroleum Reserve.
ΔT is the temperature change, °C.
t is time, s.
$t_{2\alpha-1}$ is the concentration time for algae of specified size traversing a fractional distance (corresponding to 2α-1) between the standing wave anti-node and node, s.
$t_{0.9947}$ is the concentration time for algae of specified size traversing 99.47% of the distance between the standing wave anti-node and node, s.
U_{App} is the applied voltage, V.
USH is Ultrasonic Harvester.
$v(x)$ is the velocity of a cell in an acoustic standing wave at position x along the axis of propagation, m/s.
v_{Feed} is the algal water velocity in the feed pipe or harvester, m/s.
v_g is the terminal settling velocity of the algae in the media environment under gravity, m/s.
$v_{g,\ Actual}$ is the terminal settling velocity of the actual or representative algae, m/s.
$v_{g,\ Master}$ is the terminal settling velocity of the particles represented by the master centrifuge performance curve, m/s.
x is the position along the axis of propagation for the compression wave, m.
$\widetilde{Y}$ is the mass ratio of algae to media, kg (dry weight) of algae/kg.

Greek Symbols

α is a number close to unity and is related to the fractional distance between an anti-node and node in an ultrasonic standing wave field, dimensionless.
β is the ratio of algae density to media density, dimensionless.
γ is the ratio of the speed of sound of algae to speed of sound of the media, dimensionless.
$\eta_{Centrifuge}$ is the centrifuge efficiency factor for scale up, dimensionless.
η_{Eff} is the effective performance number of an acoustic harvester, dimensionless.
$\eta_{Harvesting}$ is the mass fraction of algae harvested from the algal water, dimensionless.
η_{Metal} is the (metal specific) current dissolution efficiency, dimensionless.
η_{Pump} is the pump efficiency, dimensionless.
$\mu_{Algal\ Water}$ is the viscosity of algal water, Pa s.
μ_{Media} is the viscosity of the media, Pa s.
π is the dimensionless constant approximately equal to 3.14159.
ρ_{Algae} is the density of a single algae cell, kg/m^3.
$\rho_{Algal\ Water}$ is the density of algal water, kg/m^3.
ρ_{Lipid} is the density of algal lipid, kg/m^3.
ρ_{Media} is the density of the media in the absence of algae, kg/m^3.
Σ is the area of a gravity settler of equal performance to a specific centrifuge, m^2.
Ψ is the acoustic passivity of algae, J/m^3/s.
Ψ^* is the acoustic passivity of algae, kWh/m^3/s.
ω is the rotational frequency of a centrifuge or angular frequency of an ultrasonic harvester, radians/s.

available in the algae, and when costs can be absorbed globally without affecting local economies. It is therefore our intention that the resulting paradigms and underlying energy–cost relationships presented in this monograph be of utility to the broader H&E community, and not just to those within the U.S.

One of the challenges presented while preparing this monograph comes from the different vocabularies and reference states found

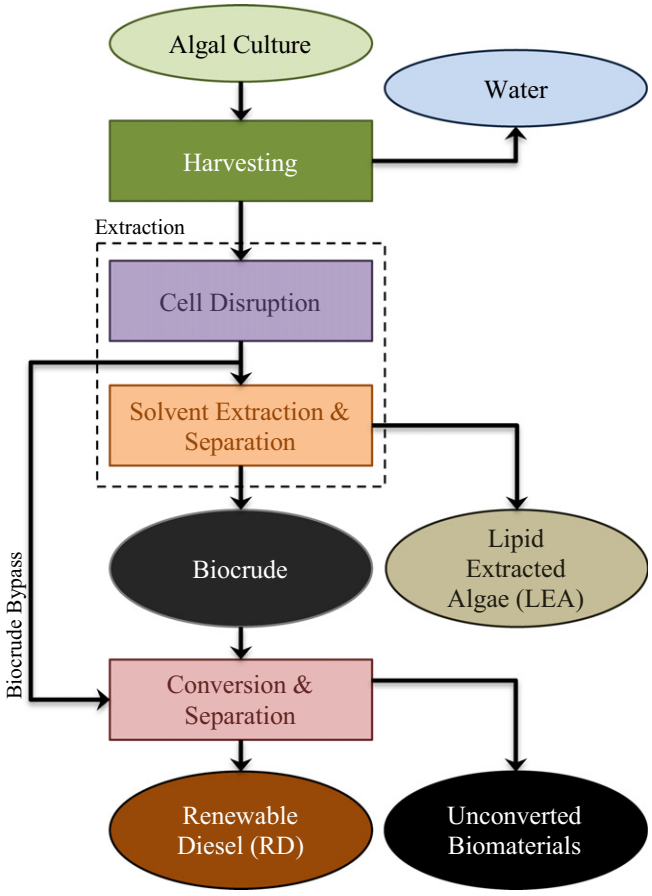

Fig. 1. Process flow diagram and nomenclature used to describe the production of renewable diesel from microalgae. Ovals represent materials and rectangles represent operations.

Table 1
Higher heating values of key liquid materials.

Material	HHV* (Btu/gal)	Volume ratio (gal/GGE)
Useful lipid	117,194[a]	1.061
RD	130,817[b]	0.9505
Gasoline	124,340[b]	1

[a] Determined from properties of the moderate condition reference state in Table 2.
[b] Obtained from [104].

throughout the algal biofuels literature. The vocabulary used in this monograph draws primarily from earlier studies describing the production of renewable diesel [6,7], and language used in the BETO multiyear program plan [2]. The technologies addressed in this monograph are limited to the harvesting and extraction sections of the renewable diesel conceptual process flow diagram in Fig. 1. Although the terms algae and algal are used throughout this monograph, the starting material is exclusively microalgae suspended in water media, be it fresh, marine, or saline water. Harvesting is generally a multistage process resulting in the concentration of algae in water. Consistent with the NABTR and NAABB terminology, extraction is used as a general term for a variety of processes that expose, concentrate, and/or separate algal lipids upstream of their conversion to renewable diesel (RD). Extraction therefore includes drying, solvent extraction, cell disruption or lysing, and solvent evaporation. Biocrude refers to the mixture of algal lipids and other biomaterials separated and concentrated typically by means of solvent extraction followed by evaporation. RD is produced by conversion of the fraction of algal lipids more specifically referred to as useful lipids, and all lipids referred to in this monograph are assumed to be useful and convertible to RD. Biofuel is a more general term that includes alcohols, alkanes, hydrogen, and diesel fuels originating from living organisms such as plants and microalgae. Conventional and cutting-edge technologies are differentiated by their state of development. Technologies referred to as conventional are more thoroughly developed with a well-established basis for scale-up and costing. Cutting-edge technologies are at an early stage of development and without accessible cost data at industrial scale. All costs are reported in units of 2011 U.S. dollars per gallon of gasoline equivalent ($/GGE), in deference to the 2022 cost metrics established by BETO [2]. Energy content in the form of the higher heating value (HHV) is the basis for volume conversions, and the values applied are listed in Table 1. HHV is equivalent to the heat of combustion when all products and reactants are at 25 °C. A complete description of the nomenclature and abbreviations used throughout this monograph is presented in the nomenclature section.

2. Harvesting costs

As with any industrial process, the total cost of harvesting algae is obtained by combining fixed-capital and product costs [8–12]. Fixed-capital costs include direct costs such as land, buildings, equipment and piping, and indirect costs such as plant design and construction. Product costs include operating costs (e.g., electrical power and raw materials), maintenance, and other costs such as overhead. A total cost comparison between harvesting technologies is beyond the scope of this monograph, but it is useful to consider the contribution that particular technologies and their scale make toward the cost of RD. Here, we compare the operational costs for cross-flow membrane filtration and electrolytic separation to the fundamental energy requirements for centrifugation and the less familiar ultrasonic harvesting in the context of the moderate condition reference state for 1st stage harvesting. This reference state is chosen for convenience, and exists within a range of conditions that creates an equivalency between 1 kWh/m^3 algal water of energy input and 1 $/GGE toward the cost of RD. This energy–cost parity simplifies the comparison of harvesting technologies to both NAABB and the 2022 BETO harvesting cost targets. Scale dependency is addressed for conventional technologies (i.e., membrane filtration and centrifugation), while more fundamental energy dependencies and limitations are described for others. A more general discussion of microalgae harvesting and related issues can be found elsewhere in the literature [13–24].

Table 2
Properties that affect the cost of algal lipid and values set for the moderate condition reference state.

Property	Units	Value	Source	Moderate condition reference state
$[B]_{Harvesting}$, the concentration of algae in the algal water at the first stage of harvesting.	$\frac{kg\ of\ Algae}{m^3\ of\ Algal\ Water}$	0.03–1.11 0.14 0.22 0.5 0.5–1.1 0.7 0.2–1.6 0.26–5	[105] [106] [107] [9] [66] [10] [14] [108]	1
$C_{Electricity}$, the cost of electricity.	$\frac{\$}{kWh}$	0.0511–0.0683 0.059 0.08 0.26	[109] [13] [9,10] [44]	0.08
$\eta_{Harvesting}$, the algal removal efficiency of the harvester.	$\frac{kg\ of\ Algae\ Harvested}{kg\ of\ Algae\ in\ Water}$	0.1–>0.9 0.28 0.8 0.9 0.95 0.65–0.95 0.92–1	[18] [110] [10] [9] [7] [13] [108]	0.8
$\hat{M}_{Lipid}$, the mass fraction of lipid in the algae.	$\frac{kg\ of\ Lipid}{kg\ of\ Dry\ Algae}$	0.05–0.64 0.09–0.72 0.10–0.15 0.11–0.63 0.17–0.61 0.25 0.25–0.58 0.35 0.457 0.5	[111] [112] [113] [105] [114] [7,9,10] [115] [66] [106] [116]	0.347
ρ_{Lipid}, the density of the algal lipid.	$\frac{kg\ of\ Lipid}{m^3\ of\ Lipid}$	850 857–892 864 920 910–925 (soybean)	[11] [113] [14] [117] [116]	864
ΔH_{Lipid}^*, the heat of combustion of the algal lipid.	$\frac{kWh}{kg\ of\ Lipid}$	8–12.75 10.55 12.2 12.72 9.39 11.8–12.8	[14,118] [66,117] [116] [81] [82] [83]	10.5
ΔH_{LEA}^*, the heat of combustion of the LEA.	$\frac{kWh}{kg\ of\ LEA}$	4.86	[66]	4.86
$\overline{E}_{Lipid}^*$, the lipid energy content in the algal water.	$\frac{kWh}{m^3\ of\ Algal\ Water}$	1.63–34 1.84	[108] [66]	3.64 at $[B]_{Harvesting}$
$\overline{E}_{Total}^*$, the total energy content in the algal water.	$\frac{kWh}{m^3\ of\ Algal\ Water}$	0.16–8.94 3.42	[105] [66]	6.82 at $[B]_{Harvesting}$

2.1. Energy–cost parity and the moderate condition

The NAABB target for harvesting is expressed in terms of the contribution toward the cost of algal lipid, which is converted to a GGE basis using the HHV values provided in Table 1. The sustainability of harvesting technologies is sometimes limited by the amount of energy required

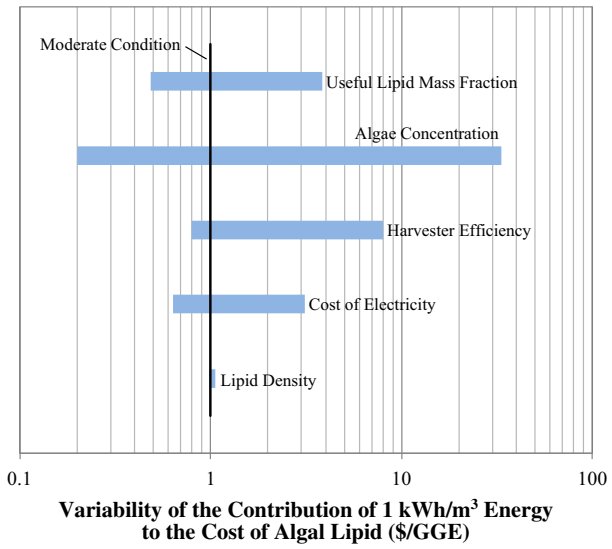

Fig. 2. The cost of 1 kWh/m^3 energy toward the cost of algal lipids using the lowest and highest values of the indicated parameters in Eq. (5). High and low parameter values were taken from Table 2.

to separate algae from a given volume of water, and at other times by known costs associated with the process. Here we construct the criterion for parity between energy requirements in units of kWh/m^3 of algal water and cost contribution in units of $/GGE and define a reference state for harvesting which is subsequently referred to as the moderate condition. We start by defining the concentration of lipid in the algal water at the time of harvest ($[L]_{\text{Harvesting}}$).

$$[L]_{\text{Harvesting}} = [B]_{\text{Harvesting}}\hat{M}_{\text{Lipid}} \tag{1}$$

Throughout this monograph, certain variables are embellished to indicate their base unit. A hat (ˆ) is used for the base unit of kg of (dry) algae, a bar (¯) for m^3 of algal water, and a tilde (˜) to indicate kg of water or media. So for example, the mass ratio $\hat{M}_{\text{Lipid}}$ in Eq. (1) has units of kg lipid per kg (dry) algae. All variables are represented in SI units, with the exception of variables denoted with an asterisk (*). The asterisk is an indicator of non-SI units unique to energy–cost parity or in some instances, non-SI units chosen for convenience. The quantity of energy derived from the lipid in kWh per m^3 of algal water ($\bar{E}^*_{\text{Lipid}}$) is given by the following.

$$\bar{E}^*_{\text{Lipid}} = [L]_{\text{Harvesting}}\Delta H^*_{\text{Lipid}} \tag{2}$$

The lipid heat of combustion, $\Delta H^*_{\text{Lipid}}$, is the lipid HHV divided by the lipid density. Losses are incurred when algae cells enter the harvester and avoid the concentrated algae stream. For the purpose of cost contribution, it is more pertinent to know the available lipid concentration and the available lipid energy, which accounts for losses incurred during the harvesting process.

$$[L]^{\text{Available}}_{\text{Harvesting}} = \eta_{\text{Harvesting}}[L]_{\text{Harvesting}} \tag{3}$$

$$\bar{E}^{\text{Available},*}_{\text{Lipid}} = \eta_{\text{Harvesting}}\bar{E}^*_{\text{Lipid}} \tag{4}$$

All harvesting processes require electrical energy, $\bar{E}^*$, which is defined as the energy input in units of kWh/m^3 of algal water. The contribution of this energy toward the price of the recovered algal lipid (C^*_{Lipid}) in units of $/GGE is given by the following.

$$C^*_{\text{Lipid}} = \left(\frac{3.785\times10^{-3}\ \text{m}^3\ \text{of Lipid}}{\text{gallon of Lipid}}\right)\left(\frac{HHV^*_{\text{Gasoline}}}{HHV^*_{\text{Lipid}}}\right)\left(\frac{\rho_{\text{Lipid}}C^*_{\text{Electricity}}}{[L]^{\text{Available}}_{\text{Harvesting}}}\right)\bar{E}^* \tag{5}$$

The first two bracketed terms appear for the purpose of unit conversions. This energy–cost relationship becomes much simpler when the

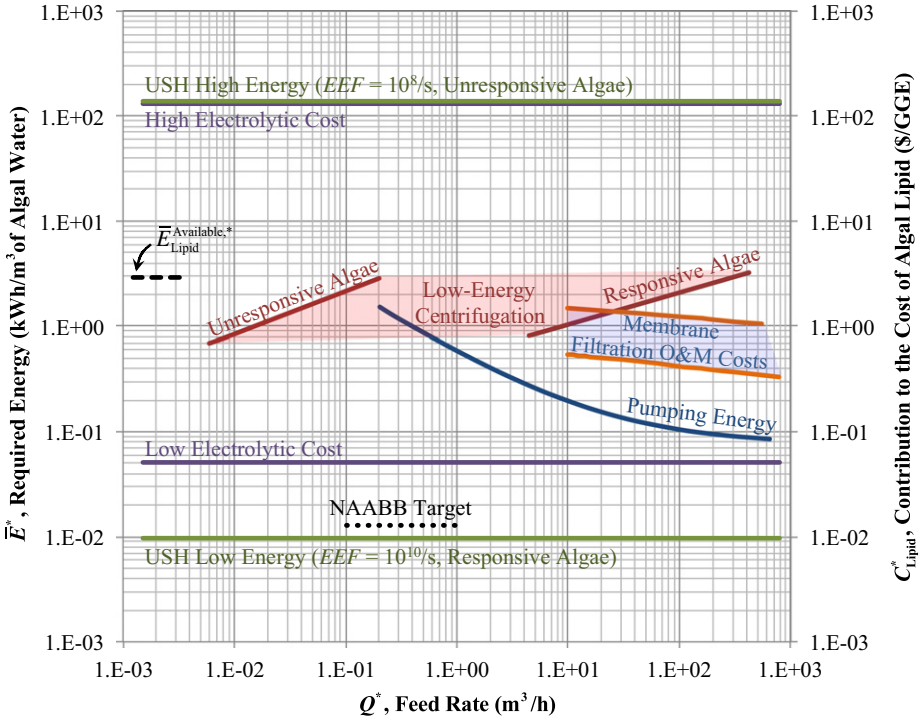

Fig. 3. A comparison of 1st stage harvesting technologies with feed water characterized by the moderate condition reference state. At this condition, the magnitude of the energy requirements and cost contribution in the units indicated are in parity.

magnitude of C^*_{Lipid} in units of $/GGE is equivalent to $\overline{E}^*$ in units of kWh/m^3 of algal water, which occurs whenever the following parity criterion is met.

$$\left(\frac{\rho_{Lipid} C^*_{Electricity}}{\eta_{Harvesting}[B]_{Harvesting}\hat{M}_{Lipid}}\right) \times \left(\frac{HHV^*_{Gasoline}}{HHV^*_{Lipid}}\right) \cong 264\left[\frac{\$\left(\text{m}^3 \text{ of Water}\right)(\text{gallon of Lipid})}{\text{kWh } (\text{m}^3 \text{ of Lipid})(\text{gallon of Gasoline})}\right] \quad (6)$$

As shown in Table 2, the properties in the first bracketed term of Eq. (6) vary significantly between investigators. However, regardless of the property values, every 1 kWh/m^3 of electrical energy consumed contributes exactly 1 $/GGE toward the cost of algal lipid as long as Eq. (6) is maintained. While parity is achieved under a broad range of conditions, the property values listed in the last column of Table 2 were selected to define the moderate condition reference state. The parameter values are generally mid-range and were chosen for reasons of simplicity. The sensitivity of the cost contribution of 1 kWh/m^3 of electrical energy to the properties and costs in the first bracketed term of Eq. (6) is shown in Fig. 2. The concentration of algae is the largest source of uncertainty, varying by more than two orders of magnitude. The moderate condition reference state describes the properties of the algal water used as feed for all 1st stage harvesting technologies in this monograph, as well as values applied for the cost of electricity and harvester efficiency. It also provides a reference for both $\overline{E}^{Available,*}_{Lipid}$ (2.91 kWh/m^3 of algal water) and the total energy content ($\overline{E}^*_{Total}$) needed to evaluate extraction technologies. The reference value of $\overline{E}^{Available,*}_{Lipid}$ is shown in Fig. 3, where the units of energy and cost are aligned in accordance with the parity criterion.

The relationship between energy input required for energy–cost parity ($\overline{E}^*$) and the energy input in SI units ($\overline{E}$) results from a simple unit conversion.

$$\overline{E}^* = \left[\frac{\text{kWh}}{3.6 \times 10^6 \text{ J}}\right]\overline{E} \quad (7)$$

Some harvesting technologies include costs that are more conveniently reported or calculated as $\overline{C}$, in units of $/m^3 of algal water. The cost contribution in $/GGE is determined using the following expression.

$$C^*_{Lipid} = \left(\frac{3.785 \times 10^{-3} \text{ m}^3 \text{ of Lipid}}{\text{gallon of Lipid}}\right)\left(\frac{HHV^*_{Gasoline}}{HHV^*_{Lipid}}\right)\left(\frac{\rho_{Lipid}}{[L]^{Available}_{Harvesting}}\right)\overline{C} \quad (8)$$

Applying properties from Table 1 and the moderate condition in Table 2, the proportionality constant in Eq. (8) becomes fixed.

$$C^*_{Lipid} = \left(\frac{12.5 \text{ m}^3 \text{ Algal Water}}{\text{GGE}}\right)\overline{C} \quad (9)$$

Now that the framework for energy–cost comparisons has been defined, we begin to contemplate harvesting technologies.

2.2. Pond transport

Before exploring the costs of different harvesting technologies, the energy requirements associated with pumping algal water from a large reservoir to an overhead tank are considered. Such a tank could be located at a harvesting facility adjacent to a network of cultivation ponds, and feed algal water gravimetrically to any choice of harvesting technology. With this design, we are transporting the pond to the harvester. It is informative to consider the cost of pond transport as some harvesting technologies may not require a conventional feed stream and their placement in the pond could also reduce costs. For the purpose of calculating energy requirements, we follow the procedure described by Peters and Timmerhaus ([8], see page 516) with the following assumptions:

a) The algal water is pumped to an overhead feed tank located 300 m horizontally from the feed pipe inlet and 11 m vertically.

$$L_{Horizontal} = 300 \text{ m} \quad (10)$$

$$L_{Vertical} = 11 \text{ m} \quad (11)$$

Sensitivity of the energy requirements to horizontal and vertical length of piping is low at the highest flow rates considered. Sensitivity values can be found in the supplementary material (see Appendix A).

b) Feed pipe internal diameters (D_{Pipe}) ranging from 6.83×10^{-3} to 0.387 m are considered, depending on the flow rate desired.

c) The average velocity (v_{Feed}) of the algal water in the feed pipe is fixed at 1.52 m/s, independent of pipe diameter. This velocity is within the recommended range of 1 to 3 m/s (see pg 526, Table 3 in [8]). The effect of velocity on energy requirements is provided in the supplementary material (see Appendix A).

d) The flow rate for a given pipe size is calculated from the average velocity and pipe cross sectional area.

$$Q_{Feed} = v_{Feed}\left(\pi D^2_{Pipe}/4\right) \quad (12)$$

e) The friction factor is calculated from Moody's equation for commercial steel [25], which is accurate to within ±5% for Reynolds numbers (N_{Re}) between 4000 and 10^7 and pipe diameters larger than 4.5×10^{-3} m.

$$f_{Friction} = 0.001375\left[1 + \left(\frac{0.9 \text{ m}}{D_{Pipe}} + \frac{10^6}{N_{Re}}\right)^{1/3}\right] \quad (13)$$

$$N_{Re} = \frac{D_{Pipe} v_{Feed} \rho_{Algal\ Water}}{\mu_{Algal\ Water}} \quad (14)$$

$\mu_{Algal\ Water}$ is the viscosity of algal water, set to 10^{-3} Pa s, and $\rho_{Algal\ Water}$ is the density of algal water, set to 999 kg/m^3. This is representative of algae in fresh water. Algae are also grown in seawater media, which has a density about 2.5% higher than freshwater, and will require similarly higher levels of energy per unit volume to pump.

f) The feed pipe includes two gate valves and three 90° elbows, which contribute the following effective length (L_e) to the feed pipe for frictional loss considerations:

$$L_{e,\ 2\ gate\ valves\ +\ 3\ \times\ 90^\circ\ elbows} = 110 D_{Pipe} \quad (15)$$

g) The pump(s) used to flow algal water through the feed line and up into the feed tank has an efficiency of 40%.

$$\eta_{Pump} = 0.4 \quad (16)$$

For a given pipe diameter, the energy input per unit volume of water required for pumping becomes,

$$\overline{E}_{Pump} = \frac{P_{Pump}}{Q_{Feed}} = \left[\frac{2 f_{Friction} v^2_{Feed}(L_{Horizontal} + L_e + L_{Vertical})}{g_c D_{Pipe}} + L_{Vertical}\right]\frac{\rho_{Algal\ Water} g_c}{\eta_{Pump}}, \quad (17)$$

and is converted to $\overline{E}^{*}_{\mathrm{Pump}}$ using Eq. (7). The pumping scheme would only be employed if the required energy was a small fraction of the available energy in the algal water and if pumping costs do not contribute significantly to the cost of algal lipid. As shown in Fig. 3, the energy required to pump algal water into the hypothetical overhead feed tank is around 1.5 kWh/m^3 at the lowest flow rate considered, which is more than half the available lipid energy under the moderate condition. As D_{Pipe} and Q_{Feed} increase, frictional losses decrease and the pumping energy approaches 0.08 kWh/m^3 at 10^3 m^3/h. At the highest flow rate considered, $\overline{E}^{*}_{\mathrm{Pumping}}$ consumes around 3% of the available lipid energy. While the energy fraction is much lower, the cost contribution of $0.08/GGE is almost an order of magnitude higher than NAABB's targeted harvesting cost. NAABB's target is so low that it virtually requires placement of the harvester in the pond. Now that the cost of feeding a harvester has been explored, we can focus on the energy requirements and costs resulting from the choice of harvesting technology.

2.3. Membrane filtration

Filtration has been used for centuries to treat water and is considered among the least costly of conventional technologies for concentrating algae. Pressurized water is forced through a filter where algae accumulate as a filter cake. This is typically not very effective as flexible algae cells and other organic materials foul the filters and reduce the flow of water [26]. Cross flow membrane filtration reduces the accumulation of filter cake by circulating water at a high velocity tangentially across the filter while maintaining sufficient pressure to force some water through the filter. As the concentration of algae increases in the circulating system, permeation decreases [27] requiring periodic discharge of the concentrate and purging/cleaning of the membranes. Here we consider operating and maintenance (O&M) costs derived from the energy required for water circulation and membrane purging, chemical costs for membrane cleaning and washing, equipment maintenance, and membrane replacement. Filtration [26,28,29] and cross flow membrane filtration [27,30–34] have been investigated at laboratory scale for the purpose of harvesting algae, but no data exist on actual O&M costs for algae harvesting at an industrial scale. And while costing tools are available for application to drinking water treatment processes [35–37], they are expected to predict lower than actual costs with algae as higher working pressures and more frequent cleaning and maintenance are anticipated with high biomass concentrations. Membrane O&M costs shown in Fig. 3 are bounded from two different correlations following adjustment to 2011 dollars via the Chemical Engineering Plant Cost Index (CEPCI) [38] (see the supplementary information in Appendix A for details). The lower bound is taken from the low-flux correlation of Vickers [36] with equipment maintenance costs added in.

$$\overline{C}_{\mathrm{Membrane,\ Low}} = 0.057\left(Q^{*}\right)^{-0.115} \tag{18}$$

Q^* is the capacity of the water treatment plant in units of m^3/h of algal water. This correlation assumes year-round operation at full design capacity, which drives costs down. The upper bound is taken from U.S. EPA cost estimates [37] adjusted to 2011 dollars.

$$\overline{C}_{\mathrm{Membrane,\ High}} = 0.147\left(Q^{*}\right)^{-0.088} \tag{19}$$

EPA cost estimates are based on operations at 20 to 70% capacity and are in close agreement with the actual cost data reported by Adham et al. [35] when labor costs are included. Derivation of Eqs. (18) and (19) as well as the comparison to the data of Adham are provided in the supplementary information (see Appendix A). Eqs. (18) and (19) are applicable at flow rates between 10 and 10^3 m^3/h. Eqs. (9), (18), and (19) were used to create the bounded membrane filtration costs shown in Fig. 3. Danquah et al. [32] measured the pump energy for cross flow membrane filtration with *Tetraselmis suecica* at a slightly lower concentration of biomass (0.6 kg/m^3) than the moderate condition. The energy requirements were around 2 kWh/m^3 at permeation rates between 0.032 and 0.046 m^3/h. While Danquah's flow rates are lower than the applicable range of Eqs. (18) and (19), the cost contribution to algal lipid under the parity condition ($2/GGE) is well above the NAABB target for harvesting costs without considering anything more than power requirements. Loss of algae in filtration processes is not always reported by investigators, but Petrusevski et al. [31] reported losses as high as 40% depending on the algae species and concentration factor.

2.4. Electrolytic separation

Electroflocculation and electrocoagulation processes have been applied to harvest both freshwater [39–42] and marine [42–44] algae. While some authors attempt to differentiate between these processes, electrode materials and operating conditions used are similar and raise questions about the exclusivity of the underlying mechanisms. Both processes can use electrolysis to produce hydrogen gas at the cathode and oxygen gas at the anode. Electroflotation occurs when gas bubbles attach to algal flocs and force them to rise to the water surface [40]. In some applications, the flocs settle to the bottom of the vessel by avoiding the gas bubbles or by avoiding conditions that produce gas.

Table 3
Electrolytic studies aimed at harvesting or removing algae.

Source	Algae	Freshwater or marine	$[B]_{\mathrm{Harvesting}}$ Algae concentration (kg/m^3)	I/Q^* Current to flow rate ratio (A h/m^3)	Vessel volume & process description	Electrode material	U_{App} Applied voltage (V)	Metal Concentration
[39]	*Scenedesmus acutus* (80%) and *Chlorella vulgaris* (20%)	Freshwater	0.283	50 to 79	1 L, Batch	Al	10–30	Not measured
[40]	Blue-green and green algae and diatoms	Freshwater	Circa .0045 to .036	11 to 23	100 L, Batch	Pb & Al	18–85	Not measured
[41]	*Microcystis* species	Freshwater	Circa 0.075 to 0.5	21 to 100	1 L, Batch 1.2–12 L, Continuous	Ti & Al	14–75	0.2–1 ppm [Al]
[42]	*Chlorella vulgaris* (F) & *Phaeodactylum tricornutum* (marine diatom)	Freshwater & Marine	0.3 to 0.6	250 to 400 (F) 50 to 100 (Salt)	1 L, Batch	Ir/Ti, Al, Fe	1–40	Circa 2 ppm [Al] in fresh water Circa 0.4 ppm [Al] in salt water 1–2% of biomass
[119]	*Chlorococcum* & *Tetraselmis* species	Marine	0.6 (*Chl*) 0.3 (*Tet*)	38 to 65 (*Chl*) 15 to 66 (*Tet*)	0.3 L, Batch	SS	3–10	Not measured
[43]	*Nannochloris oculata*	Marine	1	260 to 520	0.12 L, Continuous	Al	Circa 1	37–87 ppm [Al]
[44]	*Tetraselmis* species	Marine	Not reported, 0.25 assumed	17.2 to 34.4	4.8 L, Batch	Al	5–5.3	Not measured

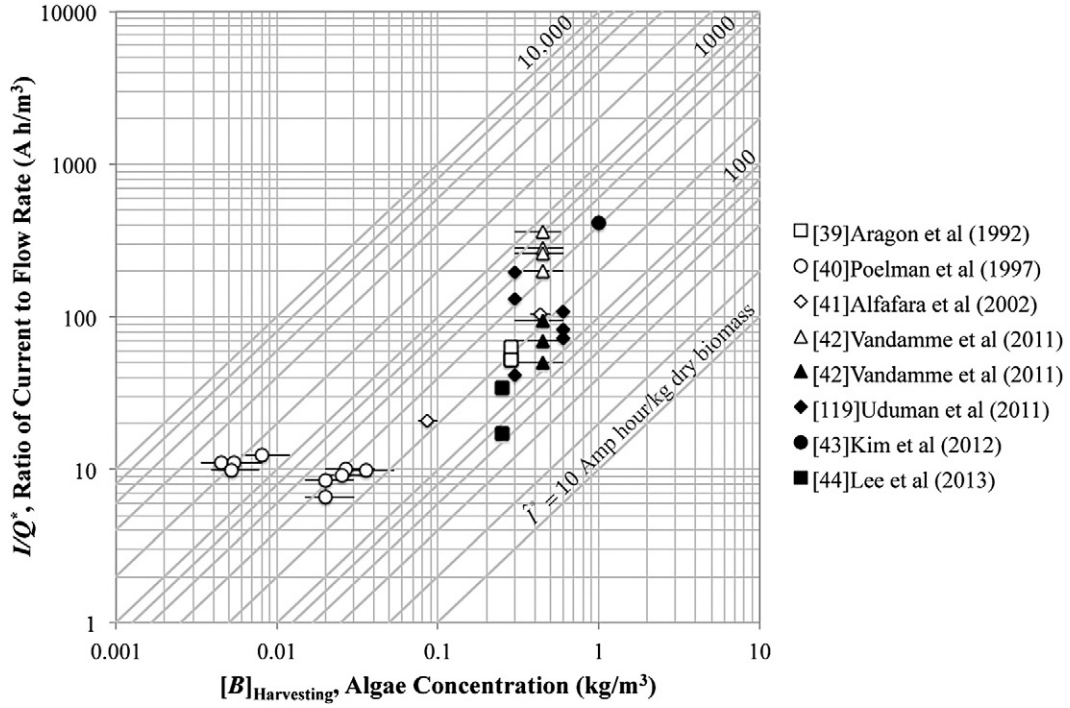

Fig. 4. A survey of conditions applied for the removal of algae from wastewater using electrolytic separation technologies. Open and closed symbols represent freshwater and marine species of algae, respectively.

Hydroxyl ions are coproduced at the cathode, which increases the pH of the algal water and contributes to chemical erosion of the cathode [45]. Electroflocculation [40] has been described as a process by which negatively charged algal cells are attracted to the anode and electrically neutralized upon contact. In this process, the anode is both electrically and chemically inert. Neutralized algae come together or self-flocculate to form large aggregates. Electrocoagulation is differentiated from electroflocculation by the oxidative dissolution of a sacrificial anode, which provides a source of polyvalent metal cations that form large flocs and entrap the algae cells. Both aluminum and iron sacrificial anodes have been used, but aluminum anodes were found to have superior removal rates [42] and are often used in processes that are described as electroflocculation or electrocoagulation processes. A list of published electrolytic studies that have removed or harvested microalgae is provided in Table 3. The operating costs considered here are derived from electricity and electrode consumption [46].

$$\overline{C}_{\text{Electrolytic}} = \left(\frac{C^*_{\text{Electricity}} U_{\text{App}}}{10^3 \ \text{W/kW}} + \dot{D}^*_{\text{Metal}} \, C_{\text{Metal}} \eta_{\text{Metal}} \right) \hat{I}^* [B]_{\text{Harvesting}} \tag{20}$$

C_{Metal} is the cost of the anode metal in \$/kg, $\dot{D}^*_{\text{Metal}}$ is the anode metal dissolution rate in kg/A h, $\hat{I}^*$ is the specific charge of the algal biomass in units of A h/kg of dry biomass, which is related to the current, flow rate, and algae concentration.

$$\hat{I}^* = \frac{I}{Q^* [B]_{\text{Harvesting}}} \tag{21}$$

U_{App} is the applied voltage, and η_{Metal} is the current dissolution efficiency. Similar equations for electrolytic operating costs [44,46] contain a dependence on the ratio of electrical current to algal water flow rate (I/Q). However, as shown in Fig. 4, the I/Q^* ratio is dependent on the biomass loading, which varies broadly among investigators. Alfarara et al. [41] reported lower aluminum values in the water while operating at no higher than 0.07 A h/mg chlorophyll *a*, which for *Microcystis aeruginosa* [47] is estimated to be equivalent to $\hat{I}^*$ values between 200 and 300 A h/kg of biomass. By inserting into Eq. (20) \$0.08/kWh for the price of electricity, an aluminum dissolution rate of 3.356×10^{-4} kg/A h as determined from Faraday's Law, and the 2011 average price of aluminum of \$2.56/kg [48], the operating cost of electrolytic systems using aluminum electrodes is obtained.

$$\overline{C}_{\text{Electrolytic}} = \frac{\left(0.08 U_{\text{App}} + 0.859 \eta_{\text{Metal}}\right)}{1000} \hat{I}^* [B]_{\text{Harvesting}} \tag{22}$$

The applied voltage depends on the circuit resistance, which in one freshwater application doubled approximately every 25 days in the absence of maintenance [46]. Values of applied voltage taken from the literature (see Table 3) ranged from 1 to 85 V. The current dissolution efficiency is zero when inert anodes and cathodes are used, as low as one when an aluminum anode is used with an inert cathode [45], and as high as 2.5 when both anode and cathode are made from aluminum [45,46]. The operating costs of electrolytic processes were bounded by using Eq. (22) along with applied voltages of 1 and 50 V, current efficiencies of 0 and 2.5, $\hat{I}^*$ values of 50 and 2000 A h/kg of dry biomass, and the value of $[B]_{\text{Harvesting}}$ as defined by the moderate condition. The contributions to the cost of algal lipid were then calculated using Eq. (9), and are shown in Fig. 3 as lower and upper bounds. The cost contribution to algal lipid from electroflocculation processes operating with inert electrodes could be significantly lower than membrane filtration. Unlike other harvesting technologies, the cost contribution is unaffected by the concentration of algae in the algal water, as the concentration term in Eq. (22) and imbedded in Eq. (9) cancel each other. The only way to affect the cost contribution is by changing the cost values imbedded in Eq. (22) or by changing the mass fraction of lipid in the harvested algae.

2.5. Centrifugation

It is desired to represent the specific energy–feed rate relationship for different types of sedimentation centrifuges and for different

Table 4
Properties of micro-organisms and media that determine responsiveness to centrifugation and ultrasonic harvesting.

Matter	d Cell diameter (μm)	ρ Density of a cell or media (kg/m^3)	ρ-ρ_{Media} Cell excess density (kg/m^3)	v_g Settling velocity (μm/s)	c Cell speed of sound (m/s)	K_S Acoustic contrast	$\overline{P}_{Algae}$ (MW/m^3)	Ψ^* Cell passivity (kWh/m^3/s)
Microalgae	2.8[a], 3.8[p] (3.8–11.4)[b], (4–10)[c]	1100[a], 1050[p] (1020–1050)[n] (1020–1250)[c]	94[a] (10–300)[j]	0.8[a], (−3 to 12)[k], (<3)[l], (0.3 to 7.3)[m]	1540[a], (1500–1628)[d]	0.073[a]	18.85[a]	(9.1×10^8)[a]
Zooplankton	–	(1035–1100)[e], 1064.7[h]	–	–	(1502–1555)[e], (1559–1570)[h], 1530[i]	–	–	–
Water	–	999[a]	–	–	1497[a]	–	–	–
Sea water	–	1025[f]	–	–	1521.46[g]	–	–	–
Responsive algae (in sea water)	7.78	1116	91	3	1625	0.093	14.6	9.6×10^7
Unresponsive algae (in sea water)	2.83	1027.3	2.3	0.01	1530	0.005	6.9	1.35×10^{10}

[a] *Chlorella* species and other materials reported in [120].
[b] Nominal diameters of various microalgae species reported in [54].
[c] See Table 3, pp. 20–23, for spherical algae diameters, and Table 8, p. 57, for algae density in [52].
[d] Approximate sound speed range for algae cited in [121].
[e] See [122].
[f] See [123].
[g] Seawater at 35 ppt salinity, 1 bar and 20 °C as reported in [124].
[h] Speed of sound in *Euphausia superba* from [125].
[i] Values reported in [126].
[j] See [127].
[k] See [53].
[l] Measurements on green algae [54].
[m] Measurements on diatoms [54].
[n] See [128].
[p] See [63].

properties of algae by means of a master curve. That is, a curve that can be shifted in accordance with the ease or difficulty of algae separation as determined by their properties. The scale-up of centrifuges is achieved by application of sigma theory, first described by Charles Ambler in the 1950's [49,50]. The performance of a centrifuge is a function of flow rate, algal properties, and properties of the centrifuge. The following general relationship has been derived for a variety of centrifuges in which the algae and centrifuge properties are separated.

$$Q = 2v_g\Sigma \tag{23}$$

Σ is dependent only on the properties of the centrifuge and represents the area of a gravity settler of equal performance. v_g is the settling velocity of algae under gravity and corresponds to the cut-off condition, which in the form of Eq. (23) determines the size of algae whose population is evenly split between the concentrate and dilute product streams. The settling velocity is dependent on the properties of the algae at the time of harvesting. In a quiescent water environment, algae cells or particles accelerate under the force of gravity due to their buoyancy and size. This gravitational force is given by:

$$F_{Gravity} = \frac{\pi d_{Algae}^3}{6}\left(\rho_{Algae} - \rho_{Media}\right)g_c \tag{24}$$

Table 5
Data used to construct the centrifuge master curves [56].

Type of centrifuge	D Drum diameter (cm)	f Cyclic frequency (revolutions per minute)	$\overline{E}^*_{Centrifuge}$ Required energy (kWh/m^3)	Σ Equivalent area (m^2)	Q^* Flow rate (m^3/h)	$\eta_{Centrifuge}$ Efficiency factor range	$\eta_{Centrifuge}$ Efficiency factor applied
Tubular	10.48	15,000	1.88	2508	0.023–2.27	0.9[a,d]	0.9
	12.45	15,000	2.65	3902	(0.045–4.542)[§]		
	10.41	10,000	0.83	1022	(0.023–2.27)[§]	0.45[a]	0.4
Disk	24.13	6500	1.87	19,974	(1.136–11.356)[§]	0.4[c]	
	31.5	6250	2.95	39,484	(1.136–11.356)[§]	0.55[d]	
	34.8	4650	1.99	36,511	(1.136–11.356)[§]		
	49.5	4240	3.36	97,548	(4.542–45.425)[§]		
Helical Conveyor	15.24	6000	0.64	251	To 4.542	0.6[a]	0.67[‡]
	35.56	4000	1.54	1245	To 17.034	(0.62–0.67)[b]	0.67[‡]
	35.56	4000	1.54	2787	To 17.034		0.62[‡]
	50.8	3350	2.20	3716	(To 11.356)[§]		0.62[‡]
	63.5	3000	2.76	5667	To 56.781		0.67[‡]
	63.5	2700	2.24	7990	(To 56.781)[§]		0.67[‡]

[§] Values estimated by comparison of Tables 19–29 and 19–30 [56].
[‡] Values estimated by comparison of theoretical and experimental Σ values (see Table 22.1 in [129]).
[a] See Table III in [130]
[b] See [131].
[c] See [132].
[d] See [56].

When a particle settles in the surrounding media, a drag force arises opposing $F_{Gravity}$ as described by Stokes' Law [51].

$$F_{Drag} = 3\pi\mu_{Media} v_g d_{Algae} \tag{25}$$

The cell very quickly reaches a constant terminal velocity, which is obtained by equating gravity and drag forces and rearranging for v_g.

$$v_g = \frac{\left(\rho_{Algae} - \rho_{Media}\right) d_{Algae}^2 g_c}{18\mu_{Media}} \tag{26}$$

Settling velocities of live algae in quiescent environments are known to deviate from Stokes equation [52] and display complex time dependencies [53]. This is due to the non-spherical shape of some algae and a variety of mechanisms available to live algae that affect their buoyancy and mobility. Burns and Rosa [53] measured settling velocities in some freshwater algae that increased from circa 0.3 to 3 μm/s over a 6 to 12 h period. Settling velocity dynamics is not relevant in the high force fields and short harvesting times of a centrifuge, but plays a significant role in the ineffectiveness of harvesting technologies that require long residence times such as gravity settlers. Therefore, the designer needs to be mindful of the dynamic nature of algal properties and apply values to the Stokes equation that are representative at the time of harvesting. As indicated in Table 4, a wide range of settling (and sometimes rising) velocities has been reported in the literature [53–55].

The performance of a variety of centrifuges that differ in type, size and flow rate capacity is approximately described by an iso-v_g curve obtained by adjusting the flow rate to yield fixed v_g values. Eq. (23) can be rearranged and written in a more general form:

$$v_g = \frac{Q}{\eta_{Centrifuge}\Sigma} \tag{27}$$

where $\eta_{Centrifuge}$ is an efficiency factor that accounts for deviations from ideal flow and is used to compare performance between centrifuges of differing design. For a given centrifuge operating at a fixed rotational frequency and with a fixed Σ value, the flow rate fixes the cut-off v_g. In Eq. (27), we have reduced the cut-off flow rate by exactly ½ so that the yield is approaching unity and more in line with the assumed yield in the moderate condition. The instantaneous settling velocity of any given algae population is more accurately described by a distribution rather than a single value. The fraction of algae in a given population with v_g lower than the cut-off will largely pass through the centrifuge with the bulk of the water, and those with higher v_g will end up in the concentrate stream. In practice, the feed rate through a continuous centrifuge operating at a fixed rotational frequency in combination with the distribution of algal properties determines its performance. When an acceptable portion of the algae population is recovered in the concentrate stream, it may be desired to increase the flow rate. For constant performance, the processing rate can only be increased by application of centrifuges with higher Σ values.

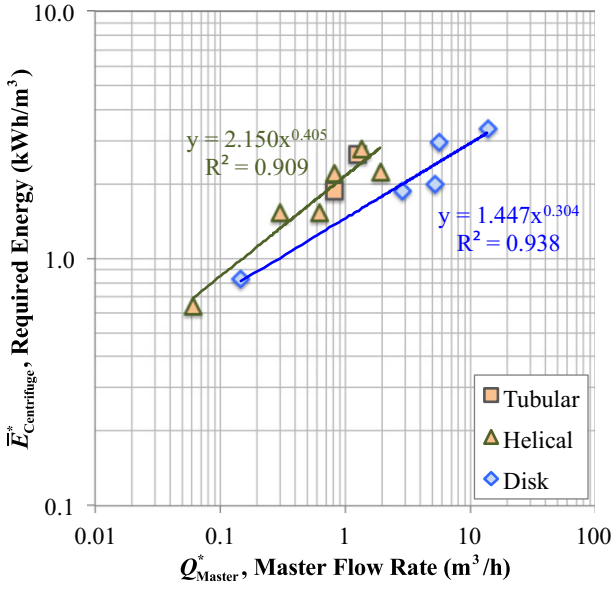

Fig. 5. Centrifuge master curves for removal of particles with a settling velocity of 0.1 μm/s. Disk centrifuges operate at higher flow rates than tubular and helical centrifuges, while achieving the same performance. The master curves shift horizontally to align with actual flow rates according to Eq. (32).

For a given centrifuge, the power requirement per unit of feed rate (P/Q) represents the energy cost per unit volume of algal water ($\bar{E}_{Centrifuge}$) and is dependent on the density of the algal water and the properties of the centrifuge.

$$\bar{E}_{Centrifuge} = \left(\frac{P}{Q}\right) = \rho_{Algal\ \ Water}\omega^2 r^2 \tag{28}$$

ω is the rotational frequency and is a function of the cyclic frequency,

$$\omega = 2\pi f, \tag{29}$$

and r is the radius of the centrifuge. Eq. (28) indicates a simple linear relationship between P and Q for a given centrifuge operating at a fixed rotational frequency. Parameters for three different types of centrifuges with throughputs that range from 0.02 to 57 m^3/h are provided in Table 5. Feed rates were adjusted within the throughput range of each centrifuge to achieve fixed v_g values ranging from 0.003 to 3 μm/s (see the supplementary information in Appendix A for details). The iso-v_g data sets obtained were shifted horizontally to achieve overlay onto the $v_{g,\ Master}$ data set corresponding to a settling velocity of 0.1 μm/s. As shown in Fig. 5, disk centrifuges operate at somewhat higher flow rates than tubular and helical centrifuges and the master curve provides the following approximate relationship between $\bar{E}^*_{Centrifuge}$ in kWh/m^3 and Q^*_{Master} in m^3/h for algae when the settling velocity is equal to $v_{g,\ Master}$.

$$\bar{E}^*_{Disk} = 1.447\left(Q^*_{Master}\right)^{0.304}, \quad \left[0.15 < Q^*_{Master} < 14\ \text{m}^3/\text{h}\right] \tag{30}$$

For tubular and helical centrifuges, the master curve is approximated by the following relationship.

$$\bar{E}^*_{Tubular\ \&\ Helical} = 2.15\left(Q^*_{Master}\right)^{0.405}, \quad \left[0.06 < Q^*_{Master} < 2\ \text{m}^3/\text{h}\right] \tag{31}$$

For algae with different settling velocities, the master curves shift horizontally to higher or lower actual flow rates according to the following equation.

$$Q^*_{Actual} = \left(\frac{v_{g,\ Actual}}{v_{g,\ Master}}\right) Q^*_{Master} \tag{32}$$

Eqs. (30) and (32) are applicable in the Q^*_{Master} range indicated and yield $\bar{E}^*_{Centrifuge}$ values between 0.6 and 4 kWh/m^3. While this range covers low-energy centrifuges, it does not include all high-capacity centrifuges. For example, Perry's Handbook [56] lists centrifuges with maximum throughputs over 170 m^3/h and $\bar{E}^*_{Centrifuge}$ values as high as 6.3 kWh/m^3.

The accuracy achieved by the master curve approach was calculated at the extremes of flow rates for each centrifuge in Table 5 and was determined to range within ±20% for all centrifuges. This level of accuracy is acceptable for the purpose of comparing centrifuge energy requirements to other separation technologies. The master curve approach makes it possible to estimate the centrifugation energy–flow

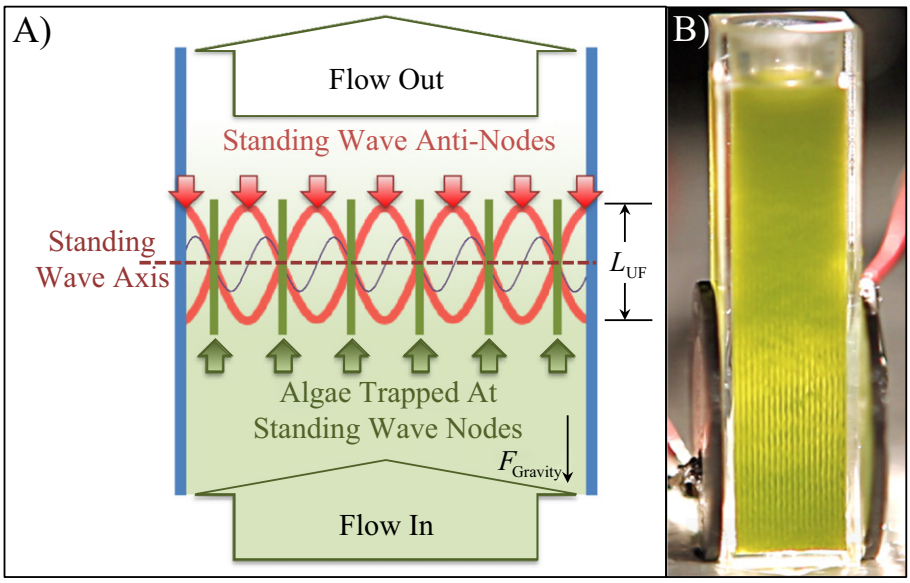

Fig. 6. A) Conceptual schematic of a flow-through ultrasonic harvester showing the dynamic standing wave (red) and the static axial primary radiation force (purple) in relation to the flow and trapped algae. The standing wave pressure has a cosine spatial dependency, which oscillates between extrema at the anti-nodes and is always zero at the nodes. The radiation force is in the positive x direction (i.e., to the right) when above the standing wave axis, and in the negative x direction (i.e., to the left) when below the standing wave axis. In this example, the radiation force drives algae from the anti-nodes to the nodes. B) A small batch ultrasonic harvester with distinct algae concentration lines. Video of this device in operation is included with the supplementary files (see Appendix A).

relationship for harvesting algae that span a range of properties. Algae that are responsive to centrifugation have properties that lead to high v_g values and visa versa. The properties of algae leading to v_g values of 0.01 and 3 μm/s for unresponsive and responsive algae, respectively, are listed in Table 4. $\overline{E}^{*}_{\text{Centrifuge}}$ curves were calculated using Eqs. (31) and (32) for unresponsive algae and using Eqs. (30) and (32) for responsive algae, and are shown in Fig. 3. While there is some overlap, the cost of centrifugation is generally higher than the cost of membrane filtration within the context of the moderate condition.

2.6. Ultrasonic harvesters

Ultrasonic harvesters function from the principle of a standing wave created by forward and reverse propagating pressure waves in a body of water [57,58], such as water that contains algae. Interaction of the standing wave with the algae cells results in primary and secondary radiation forces that move the cells closer together to form aggregates. Primary radiation forces have both axial and transverse components, where the axis of the acoustic pressure standing wave is adopted for reference. The axial component moves cells toward fixed positions along the standing wave axis (see Fig. 6). Transverse primary radiation forces assist in the trapping of cells by working against gravity, drag and other forces orthogonal to the standing wave axis [58,59]. The secondary radiation force is an intercellular force that acts between cells aligned orthogonal to the standing wave axis. In the presence of these forces, algae cells become trapped and form aggregates. When the gravitational force overcomes the drag and transverse primary radiation forces, the aggregates settle to the bottom of the harvester vessel[1] where a concentrated supply of algae is available for further processing. Woodside et al. [58] investigated the magnitude of these forces and concluded that the axial primary radiation force is much larger than transverse primary radiation forces and the secondary radiation force. Here, we focus on the axial primary radiation force to develop a design basis for ultrasonic harvesters.

The ultrasonic harvesting process starts with the transport of algae cells to fixed positions along the standing wave axis, followed by cell aggregation, and ends with the settling of aggregates. We assume that the limiting step in this process is the time required to transport cells to fixed axial positions. The axial radiation force (F_S) acting on algae in a standing wave is provided from acoustic theory [57,60].

$$F_S = \left(\frac{\pi^2 f d^3_{\text{Algae}}}{c_{\text{Media}}}\right)\langle \overline{E}_S\rangle K_S \sin\left[\left(\frac{4\pi f}{c_{\text{Media}}}\right)x\right] \tag{33}$$

$\langle \overline{E}_S\rangle$ is the time-averaged energy density of the standing wave and is a complex function of the piezoelectric and electromechanical properties of the harvester materials and power input [57,61]. K_S is the acoustic contrast of the algae and is a function of both media and algae properties.

$$K_S = \frac{1}{3}\left(\frac{5\beta-2}{2\beta+1} - \frac{1}{\beta\gamma^2}\right) \tag{34}$$

$$\beta = \rho_{\text{Algae}}/\rho_{\text{Media}} \tag{35}$$

$$\gamma = c_{\text{Algae}}/c_{\text{Media}} \tag{36}$$

According to Eq. (33), the radiation force is sinusoidal along the standing wave axis and is zero at $x = nc_{\text{Media}}/4f$ and maximum at $x = (2n-1)c_{\text{Media}}/8f$ (see Fig. 6). When the acoustic contrast is positive, algae cells are forced away from the standing wave anti-nodes toward the standing wave nodes. When the acoustic contrast factor is negative, algae cells are forced away from the standing wave nodes toward the standing wave anti-nodes. Given that the time dependency is only dependent on the magnitude of the contrast factor and not its sign, we will assume a positive acoustic contrast for the purpose of describing the radiation force effect. Applying Eq. (25) for the hydrodynamic drag force and assuming quasi-equilibrium with the radiation force, the terminal velocity of an algae cell moving toward a node is shown

[1] See the video included in the supplementary material.

to be dependent on its position along the axis.

$$v(x) = \frac{dx}{dt} = \left(\frac{\pi f d_{Algae}^2}{3\mu_{Media} c_{Media}}\right)\langle \overline{E}_S\rangle K_S \sin\left[\left(\frac{4\pi f}{c_{Media}}\right)x\right] \tag{37}$$

The closer a cell is to an anti-node, the longer it will take to reach the node, the region where cells are trapped and accumulate. Also, a cell located precisely at an anti-node experiences no radiation force, has a zero axial velocity and will never arrive at the node. Therefore, the characteristic time ($t_{2\alpha-1}$) for concentration is the time needed for an algae cell to move from an initial position very near an anti-node to a position of equivalent proximity from the adjacent node. Rearrangement and integration of Eq. (37) provides the following.

$$\begin{aligned} t_{2\alpha-1} &= \frac{3\mu_{Media} c_{Media}}{\pi f d_{Algae}^2 \langle \overline{E}_S\rangle K_S} \int_{\frac{(1-\alpha)c_{Media}}{4f}}^{\frac{\alpha c_{Media}}{4f}} \frac{dx}{\sin\left[\left(\frac{4\pi f}{c_{Media}}\right)x\right]} \\ &= \frac{6\mu_{Media}}{\langle \overline{E}_S\rangle K_S}\left(\frac{c_{Media}}{2\pi f d_{Algae}}\right)^2 \ln[\tan(\alpha\pi/2)] \end{aligned} \tag{38}$$

α is a dimensionless number close to unity and is related to the fractional distance (i.e., $2\alpha - 1$) that the cell traverses between the standing wave anti-node and node. Taking the maximum speed of sound in water to be around 1522 m/s and assuming a minimum operating frequency of 1 MHz, the maximum distance between the anti-node and node is $c_{Media}/4f$ or 381 μm. If we consider a cell 1 μm from the anti-node moving to a position 1 μm from the node, the fractional distance is 0.9947, α is equal to 0.9974, and $\ln[\tan(\alpha\pi/2)]$ is approximately 11/2. This value of α is adequate for the purpose of calculating the characteristic time of concentration in an ultrasonic harvester operating at frequencies at or above 1 MHz. By combining Eqs. (38) and (26), the concentration time to capture 99.47% of the algae of a given size can be formulated with the algae properties separate from the harvester properties.

$$t_{0.9947} \approx \left\{\frac{11 c_{Media}}{6\omega^2\langle \overline{E}_S\rangle}\right\}\left(\frac{\overline{P}_{Algae}}{v_g}\right) \tag{39}$$

$$\overline{P}_{Algae} = \frac{c_{Media}\left(\rho_{Algae} - \rho_{Media}\right)g_c}{K_S} \tag{40}$$

The responsiveness of the algae is determined by $v_g/\overline{P}_{Algae}$, which contains all of the algae properties needed to calculate the characteristic acoustic harvesting time.

$$\frac{v_g}{\overline{P}_{Algae}} = \frac{d_{Algae}^2 K_S}{18\mu_{Media} c_{Media}} \tag{41}$$

Although not commonly measured, a survey of properties is provided in Table 4 along with the values we assigned to hypothetical algae described as responsive ($v_g = 3$ μm/s, $\overline{P}_{Algae} = 14.6$ MW/m^3) or unresponsive ($v_g = 0.01$ μm/s, $\overline{P}_{Algae} = 6.9$ MW/m^3) to ultrasound and acceleration forces.

Up to this point, hydrodynamic effects present in flow-through systems have not been considered. As shown in Fig. 6, feed water is introduced into an ultrasonic harvester with an average feed velocity (v_{Feed}) orthogonal to the axis of the standing wave. The flow rate is determined by the product of the harvester area and feed velocity.

$$Q = A_{Harvester} v_{Feed} \tag{42}$$

The feed velocity affects two important elements of harvester performance; (i) in accordance with Eq. (26), it determines the size of aggregates that can settle against the direction of flow, and (ii) it determines the residence time of untrapped algae cells in the standing wave. Without knowing the cell and aggregate properties, it is impossible to specify the maximum flow rate at which loss of algae through entrainment can be avoided. A conservative range of feed velocities can be taken from sedimentation tank design, where the particle size distribution in untreated water is similar to that of algae [62]. Primary sedimentation tanks and secondary clarifiers are designed with average feed velocities (or overflow rates) between 100 and 570 μm/s, which can be taken as a lower bound for ultrasonic harvesters. Using the freshwater algae *Monodus subterraneus*, Bosma et al. [63] obtained mean separation efficiencies of 70% at feed velocities between 145 and 740 μm/s, and 17% at feed velocities near 1340 μm/s. Of course, settling of the clustered algae can also be achieved by momentary cessation of the flow and standing wave, which eliminates all concern for entrainment losses as long as the aggregates are trapped when the ultrasonic field is in place. However, if the single cell residence time in the standing wave is less than the concentration time, some portion of the algae will not have arrived at the pressure node before passing out of the standing wave. The equivalence of the residence time and the concentration time leads to the following relationship.

$$v_{Feed} = \frac{L_{UF}}{t_{0.9947}} \tag{43}$$

L_{UF} is the length of the ultrasonic field in the direction of flow. The relationship between $\langle \overline{E}_S\rangle$ and Q can be obtained by rearranging Eq. (39) in combination with Eqs. (42) and (43).

$$\langle \overline{E}_S\rangle = \frac{11 c_{Media}}{6\omega^2 L_{UF}}\left(\frac{\overline{P}_{Algae}}{v_g}\right)\frac{Q}{A_{Harvester}} \tag{44}$$

The standing wave energy density is related to the apparent power input by the effective performance number defined by Groschl [57,64].

$$\eta_{Eff} = \frac{\langle \overline{E}_S\rangle}{\overline{P}_{App}/f} \tag{45}$$

The apparent power density is the total electrical power applied to the harvester per volume of acoustic field in the algal water layer [57]. The true power density accounts for the phase angle between the voltage and driving current. The apparent power is generally greater than the true power, except when the phase angle is zero and the two are equal. The effective performance number is a complex function of the length and piezoelectric and electromechanical properties of the harvester materials through which the pressure wave travels. It can be measured experimentally and is very sensitive to the operating frequency. Combining Eqs. (44) and (45) leads to the following expression for the ultrasonic harvester P/Q ratio or required input energy.

$$\overline{E}_{Ultrasonic} = \frac{P_{App}}{Q} = \frac{\overline{P}_{App} L_{UF} A_{Harvester}}{Q} = \frac{11 c_{Media}}{24\pi^2 f \eta_{Eff}}\left(\frac{\overline{P}_{Algae}}{v_g}\right) \tag{46}$$

The separation of algal and ultrasonic harvester properties is more explicit in the following form.

$$\overline{E}_{Ultrasonic} = \frac{\Psi}{EEF} \tag{47}$$

In this simple relationship, Ψ is the passivity of the algae and is inversely proportional to the algae responsiveness. It incorporates all of the algal properties relevant to the performance of the ultrasonic

harvester.

$$\Psi = \frac{11 c_{\text{Media}}}{24\pi^2}\left(\frac{\overline{P}_{\text{Algae}}}{v_g}\right) = \frac{33 c_{\text{Media}}^2 \mu_{\text{Media}}}{4\pi^2 d_{\text{Algae}}^2 K_S} \tag{48}$$

Eqs. (47) and (48) can also be written in the units of energy–cost parity.

$$\overline{E}^*_{\text{Ultrasonic}} = \frac{\Psi^*}{EEF} \tag{49}$$

$$\Psi^* = \frac{\Psi}{3.6 \times 10^6 \text{ J/kWh}} \tag{50}$$

As shown in Table 4, Ψ^* values are around 10^8 and 10^{10} kWh/m^3/s for responsive and unresponsive algae, respectively.

EEF is the Energy Efficiency Factor and is strictly a function of the harvester design, material properties, and operating frequency.

$$EEF = f\eta_{\text{Eff}} \tag{51}$$

The *EEF* is an indicator of the effectiveness of the harvester. The upper limit is unknown, but values in the 10^9 to 10^{10} s^{-1} range have been reported [57,58] and measured in our laboratory. The input energy illustrates the importance of both algal properties and resonator design in driving down energy requirements for ultrasonic harvesting. The lowest energy input required for ultrasonic harvesting is estimated by applying a passivity corresponding to responsive algae (i.e., Ψ^* of 10^8 kWh/m^3/s) and a high *EEF* of 10^{10} s^{-1} to Eq. (47). The highest energy input required is estimated by applying a passivity corresponding to unresponsive algae (i.e., $\Psi^* = 1.35 \times 10^{10}$ kWh/m^3/s) and an *EEF* of 10^8 s^{-1}. These bounds are plotted in Fig. 3. In combination with the moderate algae condition, this leads to costs that are one to two orders of magnitude lower than conventional technologies for responsive algae and costs that are similar to conventional technologies for unresponsive algae. As improved resonator designs achieve higher *EEF* values and algae with lower passivity values are identified, the energy cost of 1st stage ultrasonic harvesting could well be lower than the NAABB target.

Unfortunately, published reports on ultrasonic harvester tests have not yet provided all of the information necessary to validate the above design basis. Bosma et al. [63] explored the performance of a small (7 ml) ultrasonic harvester over a range of conditions using the freshwater algae *M. subterraneus*, but the speed of sound of the algae and effective performance number of the harvester were not reported. The size and estimated density of the algae correspond to a settling velocity of around 0.4 μm/s. The harvester achieved a mean yield of 70% at an energy input of 14.5 kWh/m^3 and flow rate of 0.4 L/h. If we consider the settling velocity and assume a passivity of around 10^9 kWh/m^3/s, an energy input of this magnitude would require a harvester operating with an EEF of around 7×10^7 s^{-1}. Although a rough estimate, the magnitude of the EEF is low relative to the range stated above.

As algae cells concentrate under the effect of the axial primary radiation force, transverse primary and secondary radiation forces induced by the standing wave are acting to enhance cell aggregation [59]. Aggregation along the path of cell concentration increases the particle size with the effect of decreasing concentration times. Therefore, the concentration time calculated by Eq. (39) should be considered a conservative estimate, where shorter times are most likely required.

3. Extraction energy fraction

With some exceptions such as *Botryococcus braunii*, algal lipids accumulate within the cytoplasm and cell wall of algae and pose considerable challenges for low-energy removal. The isolation of lipids typically requires several formidable and energy intensive steps such as drying [65], cell disruption [66–69] and solvent extraction [66,70,71]. If the objective of the extraction process is to produce biocrude or concentrated algal lipids, then meeting the NABTR target may very well not be possible. However, if the objective is to expose lipids for the production of biodiesel, then we show that the NABTR target has already been met and that further energy savings could follow. Here we elucidate the energy requirements for various extraction processes as a function of algae concentration, using the moderate condition reference state as a basis for algal energy content. More general discussions of microalgae extraction can be found in the literature [14,15,20,22,23,65,66,70–73].

3.1. Concentration dependence

Before expanding on extraction processes, we first create the framework for energy fraction using two bounding biomass concentration dependencies. The total energy referenced by the NABTR target includes energy from both lipid and Lipid Exctracted Algae (LEA) at the extraction condition.

$$\overline{E}^*_{\text{Total}} = \overline{E}^*_{\text{Lipid}} + \overline{E}^*_{\text{LEA}} \tag{52}$$

$$\overline{E}^*_{\text{Lipid}} = [B]_{\text{Extraction}} \hat{M}_{\text{Lipid}} \Delta H^*_{\text{Lipid}} \tag{53}$$

$$\overline{E}^*_{\text{LEA}} = [B]_{\text{Extraction}} \left(1 - \hat{M}_{\text{Lipid}}\right) \Delta H^*_{\text{LEA}} \tag{54}$$

ΔH^*_{LEA} is the energy content of the LEA, which is everything in the dry algae that does not separate with a solvent. The total energy is directly proportional to the biomass concentration at the extraction condition, which can be simplified by substituting Eqs. (53) and (54) into Eq. (52).

$$\overline{E}^*_{\text{Total}} = \left\{\hat{M}_{\text{Lipid}}\left(\Delta H^*_{\text{Lipid}} - \Delta H^*_{\text{LEA}}\right) + \Delta H^*_{\text{LEA}}\right\}[B]_{\text{Extraction}} \tag{55}$$

For algae with properties described by the moderate condition in Table 2, the total energy as a function of algae concentration becomes:

$$\overline{E}^*_{\text{Total}} = \left[\frac{6.82 \text{ kWh}}{\text{kg (dry) algae}}\right][B]_{\text{Extraction}} \tag{56}$$

When $[B]_{\text{Extraction}}$ is equal to $[B]_{\text{Harvesting}}$, the total energy is equal to 6.82 kWh/m^3 of algal water. Excluding measurement error in $[B]_{\text{Extraction}}$, uncertainty in the total energy calculated from Eq. (56) is dominated by two parameters; the useful lipid mass fraction and the lipid heat of combustion. Given the range of their values in Table 2, the total energy is expected to be accurate to within ±31% due to lipid mass fraction uncertainties and to within ±13% due to uncertainties in the lipid heat of combustion.

At dilute algae concentrations, mechanisms acting on the bulk media (e.g., heating of the water) have energy requirements dependent on the volume of media processed and independent of algae concentration. Working from Eq. (56), the energy fraction (F_{Energy}) for these processes is given by the following expression.

$$F_{\text{Energy}} = \frac{\overline{E}^*_{\text{Extraction}}}{\overline{E}^*_{\text{Total}}} = \frac{\overline{E}^*_{\text{Extraction}}}{\left[\frac{6.82 \text{ kWh}}{\text{kg (dry) algae}}\right][B]_{\text{Extraction}}} \tag{57}$$

It is apparent here that uncertainties in the total energy transfer directly to uncertainties in the energy fraction. Concentration independent technologies that energize the bulk media are by their nature inefficient and achieve more favorable fractional energies by increasing $[B]_{\text{Extraction}}$. In Fig. 7, these concentration-independent processes track along the diagonal lines of constant $\overline{E}^*_{\text{Extraction}}$. However, as the concentration of algae increases, bulk properties of the

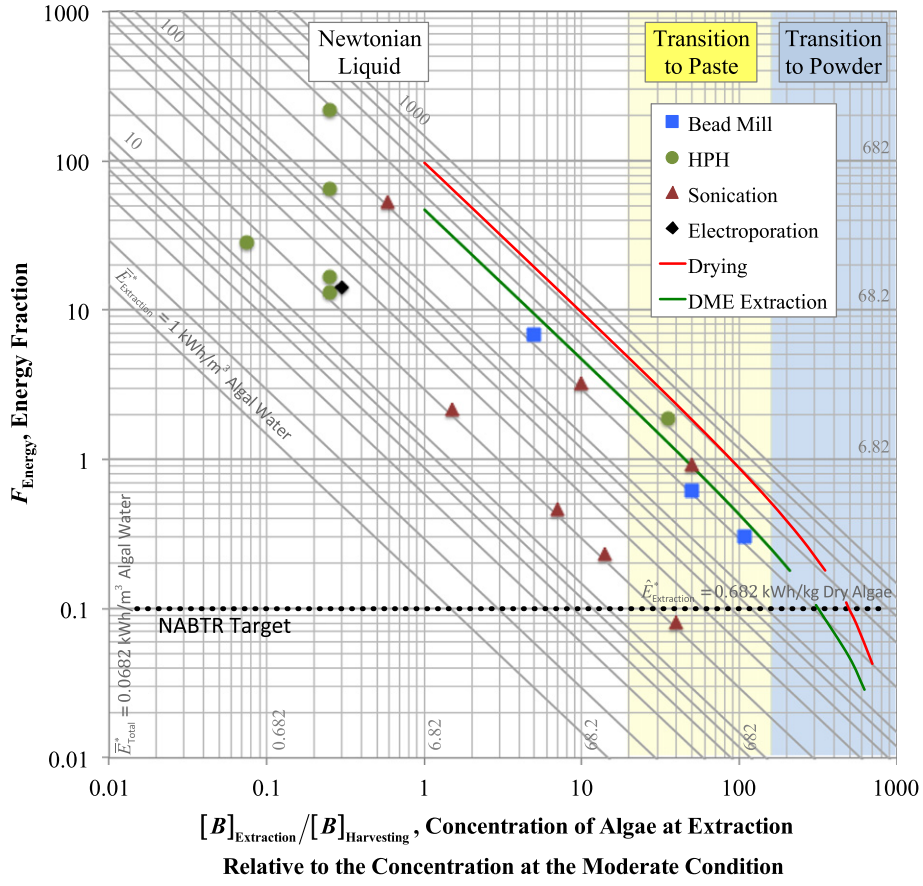

Fig. 7. Energy requirements for extraction technologies referenced to the energy content of algal water in the moderate condition reference state. Sources of data are provided in Table 7. Technologies that track along the diagonal lines (e.g., bead mill and sonication disruption technologies) display concentration independent energy requirements. Technologies that track along horizontal lines display first order concentration dependence. Sonication is the only extraction technology to have exceeded the NABTR performance target.

cellular suspension change. There are two important transitions that occur in the high algae concentration domain. Wileman et al. [74] measured the rheological properties of algal slurries and although dependent on the species of algae, observed the onset of non-Newtonian behavior at circa 20 kg/m^3. While the algal suspension may not yet be paste-like at this concentration, mechanisms that rely on rheological properties will be increasingly affected as the biomass concentration increases beyond this value. At extreme concentrations (e.g., when the algae are drying or dehydrating), continuity of the media phase breaks down. Few studies have reported water-algae isotherms [75–77], but the results indicate that dehydration could begin at concentrations as low as 167 kg/m^3. These approximate transition regions are shown in Fig. 7 with colored backgrounds.

Now imagine an extraction technology that requires a fixed quantum of energy for every algae cell in its active volume. Such technology would be highly efficient and would have energy requirements that are first order with respect to the biomass concentration.

$$\bar{E}^*_{Extraction} = \hat{E}^*_{Extraction}[B]_{Extraction} \tag{58}$$

Substitution of Eq. (58) into Eq. (57) leads to the following expression for the specific extraction energy (in units of kWh/kg of dry algae).

$$\hat{E}^*_{Extraction} = \left[\frac{6.82\ \text{kWh}}{\text{kg (dry) algae}}\right] F_{Energy} \tag{59}$$

Table 6
Thermal properties of water, common solvents, and solvent systems. All of the listed solvents are non-toxic, with the exception of chloroform/methanol.

Solvent	$\tilde{C}^*_p \times 10^3$ Heat capacity (kWh/kg solvent °C)	$\tilde{E}^*_{Vaporization}$ Heat of vaporization (kWh/kg solvent)	$\tilde{M}_{Solvent}$ Mass ratio of solvent to water	$\sum_i \tilde{E}^*_{Vaporization,i}\tilde{M}_{Solvent,i}$ (kWh/kg water)	Source
Chloroform	0.269	0.073	2.5	1.033	[80]
Methanol	0.707	0.34	2.5		
d-Limonene	0.508	0.0805	8.7	0.7	[86]
Water	1.162	0.64	1	0.64	[123]
Isopropanol	0.697	0.185	2.33	0.432	[84]
DME	0.617	0.137	2.25	0.308	[81]

When the energy fraction is unity, $\hat{E}^*_{\text{Extraction}}$ is equal to 6.82 kWh/kg dry algae. In Fig. 7, processes that have a first order dependency on cell concentration track along horizontal lines of constant $\hat{E}^*_{\text{Extraction}}$.

3.2. Drying and solvent removal

Drying and solvent distillation are energy intensive steps in any extraction process, and their preclusion or minimization is essential to assure a positive energy balance. Drying is achieved either by heating or freezing the algae and exposing it to dehydrated atmospheres, and is often performed prior to solvent extraction. Solvent removal is achieved by distillation or decompression, and the amount of solvent added is sometimes in proportion to the quantity of water in the algal paste. Therefore, the energy fraction required for drying and solvent distillation is related to the mass or volume of water in the wet algae at the extraction concentration, $[B]_{\text{Extraction}}$. Assuming the density of the wet algae is similar to that of the water media, the mass ratio of dry algae to water is roughly dependent on the algae concentration at the extraction condition.

$$\tilde{Y} \cong \frac{[B]_{\text{Extraction}}}{\rho_{\text{Media}} - [B]_{\text{Extraction}}} \tag{60}$$

The total energy available from the algae per kg of media is given by:

$$\tilde{E}^*_{\text{Total}} = \left\{ \hat{M}_{\text{Lipid}} \left(\Delta H^*_{\text{Lipid}} - \Delta H^*_{\text{LEA}} \right) + \Delta H^*_{\text{LEA}} \right\} \tilde{Y} \tag{61}$$

and the minimum fractional energy for drying becomes the following.

$$F_{\text{Drying}} = \tilde{E}^*_{\text{Vaporization}} / \tilde{E}^*_{\text{Total}} \tag{62}$$

For algae with properties similar to the moderate condition defined in Table 2, Eq. (61) becomes:

$$\tilde{E}^*_{\text{Total}} = \left[\frac{6.82 \text{ kWh}}{\text{kg water}} \right] \tilde{Y} \tag{63}$$

When the mass ratio of dry algae to water is unity, $\tilde{E}_{\text{Total}}$ is 6.82 kWh per kg of water. Approximate values of latent heats, heat capacities, and specific heats of vaporization for distillation processes are provided in Table 6. Inserting the latent heat of vaporization for water and Eq. (63) into Eq. (62), the minimum fractional energy for drying is given by the following.

$$F_{\text{Drying}} = 0.64 \text{ kWh/kg water} / \tilde{E}^*_{\text{Total}} = 0.094 / \tilde{Y} \tag{64}$$

The minimum fractional energy required to dry algae in seawater media is shown in Fig. 7 as a function of the concentration at the extraction condition. The concentration of algae at which the energy fraction falls below the NABTR target is well within the dehydrated zone. This suggests that the algal paste has to be largely dehydrated before total dehydration can be performed within the NABTR target. In addition to vaporization, drying also requires sensible heat to change the temperature of the algal water and electrical energy to flow dehydrated air, circulate heat transfer media, and operate pumps and compressors. If the paste is to be freeze-dried, then the heat of fusion (0.093 kWh/m^3) has to be added to the heat of vaporization to determine the energy fraction. The fractional energy required for sensible heat is given by:

$$F_{\text{Sensible}} = \tilde{C}^*_P \Delta T / \tilde{E}^*_{\text{Total}} \tag{65}$$

The actual energy required for drying is typically 1.3 to 5 times higher than the minimum value shown in Fig. 7 [65].

Production of algal biocrude has been achieved by solvent extraction using a variety of solvents and co-solvent systems with both dry algae [78,79] and wet algae pastes [80–86]. In a waterless extraction operation, the energy fraction is determined on a dry weight algae basis. The total energy and energy fraction becomes:

$$\hat{E}^*_{\text{Total}} = \hat{M}_{\text{Lipid}} \left(\Delta H^*_{\text{Lipid}} - \Delta H^*_{\text{LEA}} \right) + \Delta H^*_{\text{LEA}} \tag{66}$$

$$F_{\text{Energy}} = \tilde{E}^*_{\text{Vaporization}} \hat{M}_{\text{Solvent}} / \hat{E}^*_{\text{Total}} \tag{67}$$

where $\tilde{E}^*_{\text{Vaporization}}$ is the latent heat of vaporization of the solvent. As shown above, the use of dry algae is too energy intensive for biofuel production. When wet algae is used, the energy fraction is determined on a kg media basis.

$$F_{\text{Energy}} = \tilde{E}^*_{\text{Vaporization}} \tilde{M}_{\text{Solvent}} / \tilde{E}^*_{\text{Total}} \tag{68}$$

Table 7
Energy requirements reported using a variety of cell disruption technologies. See Fig. 7 for a graphical comparison of this data.

Technology	$[B]_{\text{Extraction}}$ Algae concentration (kg dry weight/m^3)	$\tilde{E}^*_{\text{Extraction}}$ Required energy (kWh/m^3)	Microalgae	% Disruption	System volume or flow rate	Source
Bead mill	5	233	*Botryococcus sp.*	–	0.1 L	[92]
	50	208	*Scenedesmus sp.*	96–100	~0.07 L	[90]
	107	220 (minimum)	*Chlorella sp.*	97	1.4 L	[91]
HPH	0.075	14.4	*Tetraselmis sp.*	95	0.2 L	[88]
	0.254	28.7	*Tetraselmis sp.*	95	0.2 L	[88]
	0.25	22.2	*Tetraselmis sp.*	95–100	10 L/h	[89]
	0.25	110.83 (minimum)	*Chlorella sp.*	95–100	10 L/h	[89]
	0.25	375	*Nannochloropsis sp.*	95–100	10 L/h	[89]
	35	444	*Nannochloris oculata*	95–100	3 L/h	[87]
Ultrasound	0.59	214	*Tetraselmis sp.*	95	0.2 L	[88]
	50	316	*Nannochloropsis oculata*	–	0.1 L	[93]
	1.5	22.2	*Chlamydomonas reinhardtii*	91–95	0.01 L	[94]
	7	22.2	*Chlamydomonas reinhardtii*	91–95	0.01 L	[94]
	14.1	22.2	*Chlamydomonas reinhardtii*	91–95	0.01 L	[94]
	40	21.92	*Schizochitrium limacinum*	circa 80	0.01 L	[94]
	10	220	*Spirulina platensis*	–	0.05 L	[95]
Electroporation	0.3	29.2	*Synechocystis sp.*	99	25 L	[97]

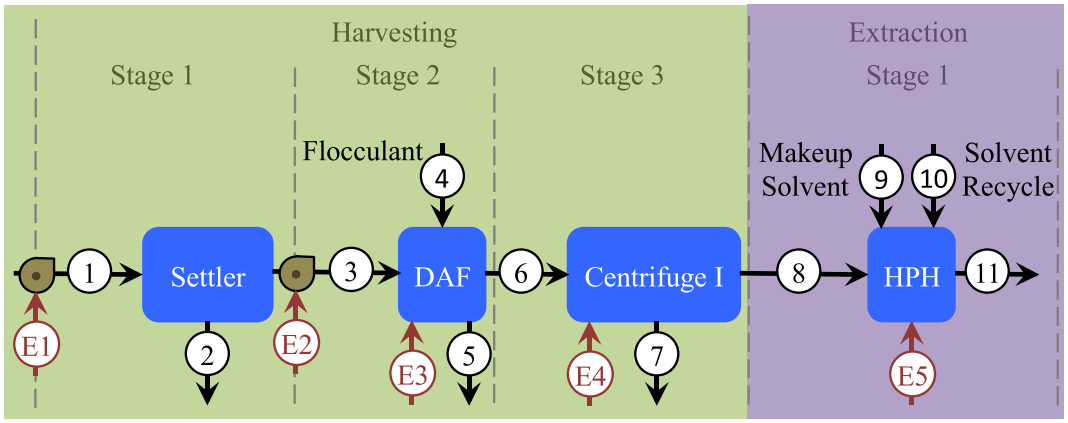

Fig. 8. The baseline H&E process (through disruption) for renewable diesel production as defined by Davis et al. [7]. Process units are shown as blue boxes. Streams are numbered for reference to Table 8. Mass streams are indicated by black arrows and energy streams with red arrows. Pumps are included in streams 1 and 3. This process transports the pond to the harvester. Harvesting is achieved in a 3 stage process that includes Dissolved Air Flotation (DAF) and disruption is achieved via High Pressure Homogenization (HPH).

The solvent system with the lowest numerator in Eq. (68) is the least energy intensive. From the values listed in Table 6, the energy requirements of the dimethyl ether (DME) system is the lowest at about half that needed to dry the algae. The normal boiling point of DME is −24 °C and the extraction is conducted near room temperature at elevated pressure. The minimum fractional energy required for DME extraction is shown in Fig. 7 as a function of the algae concentration at the extraction condition. Solvent extraction on wet algae is typically performed at concentrations of 200 kg dry weight/m^3. Even at half the energy for drying, the energy fraction for solvent extraction at this concentration is above the NABTR target.

3.3. Cell disruption

Effective cell disruption opens cell walls allowing access to intracellular lipids. The complexity and filamentous structure of algal cell walls makes them in general stronger and more difficult to disrupt than cells from other organisms [67]. A variety of mechanical technologies has been developed over the past century for cell disruption including High Pressure Homogenization (HPH) [87–89], bead mills [90–92], ultrasonic disruption or sonication [88,93–96], and electroporation [97,98]. These approaches have been reviewed previously [67,68,99,100]. Energy requirements from various investigations are listed in Table 7 and plotted in Fig. 7. Where possible, these energies correspond to non-unity fractional disruptions of at least 0.8 in an effort to quantify the minimum energy required for a given disruption technology independent of the microalgae studied. While the concentration dependence of HPH has been tested over large concentration ranges, the data shown in Fig. 7 do not track along horizontal lines and are not consistent with a first order concentration dependency. The lowest energy input for effective HPH is 14 kWh/m^3 at very dilute concentrations of *Tetraselmis*. However, this is greater than 20 times the total energy content of the algae at the dilute concentration. Even at higher concentrations, the energy fraction for HPH is greater than one. Both bead mill and ultrasonic disruption processes appear to track along diagonal lines indicative of concentration independence. Bead mill operations consume more than 200 kWh/m^3 of algal water, and even at high concentrations have not dipped below the NABTR target. Ultrasonic data are separated into two groups; a high-energy group operating around 200 kWh/m^3, and a low-energy group operating around 20 kWh/m^3. One difference between these groups is system size, with system volumes of 10 mL making up the low-energy group and system volumes between 50 and 200 mL making up the high-energy group. This suggests the question of whether ultrasound can provide similar levels of disruption at lower energy densities if delivered in increasingly confined volumes? All ultrasonic studies listed in Table 7 were conducted using ultrasonic horns. Bigelow et al. [96] employed a focused ultrasound setup whereby the compression waves propagate through a water medium and into a 1 mL enclosed volume containing the algae. This arrangement required 109 kWh/m^3 and appears to be less energy efficient than the ultrasonic horn systems. This leaves the question regarding system confinement unanswered. Published data on electroporation is particularly scant. The single study plotted in Fig. 7 indicates energy requirements similar to the low-energy sonication technology, although at relatively low biomass concentration where the energy fraction is high. Lee et al. [101,102] estimated the energy required for algae disruption to be between 0.06 and 0.25 Wh/kg of dry algae, based on the tensile strength and bond energy of the cell wall. This is equivalent to an energy fraction between (0.8 and 3) × 10^{-5}, which is well beyond the lowest energy fraction shown in Fig. 7. If the low energy ultrasonic disruption line is traced to the higher extraction concentration of 200 kg/m^3, an energy fraction less than 0.02 is achieved. This is still 1000 times higher than the theoretical limit, and speaks to the scale of inefficiency in disruption technologies. However, it is noteworthy that sonication is the only disruption technology to have dropped below the NABTR target when the moderate condition reference state is applied to represent the total energy content of the algae.

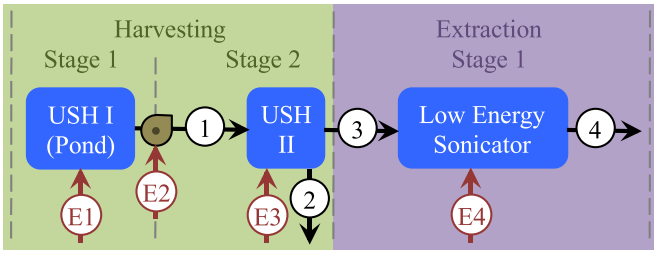

Fig. 9. An optimistic ultrasonic H&E process places the first stage ultrasonic harvester (USH) in the pond, reducing the quantity of water transported by more than an order of magnitude. Disruption is achieved via continuous sonication. See the caption of Fig. 8 for a description of symbols and Table 9 for mass and energy flow data.

4. Discussion

As a means to gauge the scale of cost and energy savings that can be achieved by an optimistic projection of ultrasonic H&E technologies,

Table 8
Mass/energy balance and operating costs for the harmonized baseline H&E process [7]. Stream numbers complement the process flow diagram provided in Fig. 8.

	Component	Unit	Stream number															
			1	E1	2	E2	3	E3	4	E4	5	6	7	E5	8	9	10	11
			Harvesting												Extraction			
Steady-state mass balance	Water	m^3/h	54,930.9		52,492.5		2438.3		0.0		2089.7	348.7	264.1		84.6	0.0	1.7	86.3
	Algae	kg dry weight/h	27,479.2		2747.9		24,731.3		0.0		2473.1	22,258.1	1112.9		21,145.2	0.0	0.0	2114.5
	Lipid	kg/h	0.0		0.0		0.0		0.0		0.0	0.0	0.0		0.0	0.0	5.7	4763.4
	LEA	kg dry weight/h	0.0		0.0		0.0		0.0		0.0	0.0	0.0		0.0	0.0	0.0	14,273.0
	Flocculant	kg dry weight/h	0.0		0.0		0.0		98.0		0.0	98.0	0.0		0.0	0.0	0.0	98.0
	Solvent	kg/h	0.0		0.0		0.0		0.0		0.0	0.0	0.0		0.0	243.6	105,482.4	105,726.1
Biomass power content[1]	Whole algae	kWh/h	172,294.4		17,229.4		155,064.9		0.0		15,506.5	139,558.4	6977.9		132,580.5	0.0	0.0	13,258.1
	Lipid	kWh/h	0.0		0.0		0.0		0.0		0.0	0.0	0.0		0.0	0.0	60.3	50,015.9
	LEA	kWh/h	0.0		0.0		0.0		0.0		0.0	0.0	0.0		0.0	0.0	0.0	69,366.9
Processing power input	Power	kWh/h		1375.0		269.0		3289.0		412.0				3870.0				
Operating costs[2]	Power	$/h		110.00		21.52		263.12		32.96				309.60				
	Flocculant	$/h							1165.70									
	Solvent	$/h														263.47		
	Sub-total	$/h	1593.30											573.07				
Totals	Total operating costs ($/hr):		2166.37		Total lipid produced (gallons/h):		1456.4		Cost contribution ($/GGE):		1.58							

Table 9
Mass/energy balance and operating costs for an optimistic ultrasonic H&E process. Stream numbers complement the process flow diagram provided in Fig. 9.

	Component	Unit	Stream number							
			E1	E2	1	E3	2	3	E4	4
Steady-state mass balance	Water	m3/h			2438.3		2194.5	243.8		243.8
	Algae	kg dry weight/h			21,983.3		4396.7	17,586.7		879.3
	Lipid	kg/h			0.0		0.0	0.0		4176.8
	LEA	kg dry weight/h			0.0		0.0	0.0		12,530.5
	Flocculant	kg dry weight/h			0.0		0.0	0.0		0.0
	Solvent	kg/h			0.0		0.0	0.0		0.0
Biomass power content[1]	Whole algae	kWh/h			137,835.5		27,567.1	110,268.4		5513.4
	Lipid	kWh/h			0.0		0.0	0.0		43,856.8
	LEA	kWh/h			0.0		0.0	0.0		60,898.2
Processing power input	Power	kWh/h	24.4	269.0		21.9			536.4	
Operating costs[2]	Power	$/h	1.95	21.52		1.76			42.91	
	Sub-total	$/h			25.23				42.91	
Totals	**Total operating costs: $68.14/h**				**Total lipid produced: 1277.1 gallons/h**				**Cost contribution: $0.057/GGE**	

reference is made to the harmonized baseline process described by Davis et al. [7] shown in Fig. 8 and to the optimistic ultrasonic process shown in Fig. 9. Here we consider processing costs up to and including cell disruption using the harmonized baseline condition of 0.5 kg/m^3 algae and 25% dry weight lipid as feed water for both processes. The baseline process assumed a 90% harvester efficiency for the first two stages, 95% for the centrifuge, and 90% disruption in the homogenizer. The USH process assumes an efficiency of 80% for each harvester and 95% for disruption. All costs in the baseline study were changed from 2007 to 2011 dollars using the CEPCI and converted to a basis of $/GGE. For the USH process, the harmonized baseline condition was applied (see the supplementary information for details). The baseline process consists of three harvesting stages and one extraction stage. The contribution to the cost of algal lipid via the baseline process is $1.58/GGE, which is derived from the energy and material costs shown in Table 8. Circa 66% of the lipid cost is due to the additives (i.e., flocculant and makeup solvent). Around 10.5% of the lipid energy entering the process is consumed by the H&E technology, 12.8% when pumps are included. The algal lipids are dispersed in hexane, which will have to be removed by distillation. In contrast, the ultrasonic process described in Fig. 9 and Table 9 contributes $0.057/GGE to the cost of algal lipid, which is more than an order of magnitude lower than the baseline process. The optimistic ultrasonic process consists of two harvesting stages and a single disruption stage, which we assume are advanced designs that operate at 0.01 kWh/m^3 for harvesting and 2.2 kWh/m^3 for disruption. Only 1% of the lipid energy entering the process is consumed by the electrical needs of the USH components, and 1.5% when pumps are included. With ultrasonic harvesting, there is no impact on the quality of recycled algae or water. The exposed lipid is either dispersed in the water phase or attached to the solid biomass material, and available for conversion to biodiesel. This product stream is similar to the feed stream described by Takisawa et al. [103], in which the lipid undergoes hydrolysis and then esterification in the aqueous phase. As this process requires elevated temperatures, the overall energy requirements may be lower by achieving higher concentrations of algae in a third harvesting stage not included in Fig. 9. Ultimately, the process conditions leading to minimum energy input are best identified by a more global optimization taking into consideration everything from the state of the algae at cultivation to the conversion of lipids to biodiesel. If biomass concentrations in the pond and each stage of harvesting were represented by the moderate condition, the cost contribution would be $0.81 and $0.02/GGE for the baseline and ultrasonic processes, respectively. These costs were arrived at assuming 80% recovery per harvesting stage and 95% disruption for both baseline and ultrasonic processes. At the moderate condition, the ultrasonic process is approaching the NAABB limit for harvesting while including the cost of disruption.

The above comparison illuminates differences in operating costs, but the baseline work of Davis et al. indicates that capital costs dominate. Fully burdened costs for the H&E baseline process is $3.44/GGE, including a capital component of around 54%. Capital costs are strongly correlated to equipment costs [8], and we hypothesize that equipment costs will be in proportion to their design complexity. In other words, processes with equipment that require no moving parts and operate at normal conditions (i.e., atmospheric temperature and pressure) will lead to lower capital costs than processes with equipment that have complex moving parts and operate at high pressures and temperatures. Centrifugation and bead mill equipment require spinning components and are

at the high end of design complexity. High-pressure systems like membrane filtration and homogenization occupy a middle ground, where stress-bearing components drive up costs. Electrolytic, electroporation, and ultrasonic processes use simple equipment (e.g., electrodes and piezoelectric components), which will hypothetically translate into lower capital costs. Ultimately, accurate costing tools need to be developed or applied to test the consistency of this hypothesis.

More research needs to be conducted aimed at lowering H&E costs and meeting the 2022 BETO targets. This requires careful experiments that achieve higher efficiencies while avoiding excessive energy input, and more thorough reporting of relevant algal and harvester/extractor properties. There are many questions that when answered will eliminate much of the uncertainty surrounding this important stage in RD production. For example, what is the distribution of passivity in a population of algae and how does this change over time? Do algae become less or more passive to ultrasound when they are laden with lipid, which may decrease the cell's density while increasing it's size? Are there genetic components to passivity that can be enhanced? Is it economically viable to remove only the low-passivity segment of algae and leave the unresponsive segment for further growth or will this lead to a population of unresponsive algae? What is the distribution of cell wall strength and how does this change through the cultivation period? Does cell wall strength affect disruption energy requirements, given that current technologies use so much more energy than is needed? It is clear that much research is needed to advance the development of cutting-edge H&E technologies and drive down the cost of algal biofuels.

5. Conclusions

A number of notable results emerge from this monograph. Firstly, from a fundamental perspective, there is merit to the idea that continued development of H&E technologies could reduce H&E costs by orders of magnitude relative to today's conventional technologies. In particular, ultrasonic and electrolytic harvesting technologies show the most potential for energy and cost reduction. In addition to lower operating energy, both of these harvesting technologies can conceptually be placed in the pond enabling a shift away from the paradigm of transporting the pond to the harvester. Ultrasonic harvesting offers the additional possibility of selectively removing more responsive algae while leaving other algae behind for continued growth within the culture environment. Ultrasonic harvesting does not introduce chemicals or metals that impact the quality of water or algae and require removal. More research is needed to demonstrate the effectiveness of electroflocculation, particularly using inert electrodes. On the extraction end, while none of the disruption technologies are at the verge of achieving the theoretical low-energy limit, ultrasonic disruption has exceeded the NABTR target when the moderate condition is used as a reference state for the algae energy content. The hypothesis that H&E technologies with simple equipment such as ultrasonic, electrolytic, and electroporation processes will lead to lower capital costs is left for future studies to confirm or disprove. Secondly, more experimental investigations in which algae and equipment properties are more clearly differentiated in assessing the performance of H&E technologies at larger scale is needed. Important algae properties include cell diameter, single cell density, concentration, speed of sound, charge density, bulk modulus, and cell wall strength and their time-resolved distributions in algae populations. In addition to algae properties, the performance of ultrasonic and electrolytic harvesters should be referenced to their EEFs and specific biomass charge, respectively, as well as to the scale of the system. Centrifuge performance should be referenced to the equipment rotational frequency, radius, and feed rate, as well as to algae properties. Membrane filtration studies should also address membrane replacement costs and lifetimes, which are the predominant limitation in meeting biofuel cost targets. Standard methods of property measurement need to be established and alliances throughout the biofuels community strengthened to affect a broader understanding of needs for cost reduction. Lastly, the constructed paradigms illustrated in Figs. 3 and 7 for H&E technologies make future advancements easier to gauge. Application of the moderate condition to 1st stage harvesting in Fig. 3 provides a straightforward comparison between energy requirements and cost contributions to algal lipid, and hence addresses the sustainability of various harvesting technologies. Likewise, the concentration dependence of energy fraction as displayed in Fig. 7 is a useful paradigm to compare extraction technologies and track their advancement toward the NABTR target and sustainability.

Acknowledgment

The authors would like to acknowledge funding of this work by the U.S. Department of Energy (DOE) under Contract DE-EE0003046 awarded to the National Alliance for Advanced Biofuels and Bioproducts (NAABB), and funding provided by the DOE Bioenergy Technologies Office. The authors would also like to thank Dr. Ryan Davis of the National Renewable Energy Laboratory for the discussions related to nomenclature and conversions between fuel types.

Appendix A. Supplementary data

Supplementary data to this article can be found online at http://dx.doi.org/10.1016/j.algal.2014.08.005.

References

[1] J. Sheehan, T. Dunahay, J. Benemann, P. Roessler, A Look Back at the U.S. Department of Energy's Aquatic Species Program — Biodiesel from Algae, NREL/TP-580-24190, 1998.
[2] U.S.D.o. Energy, Bioenergy Technologies Office Multi-Year Program Plan, 2013. (http://www1.eere.energy.gov/bioenergy/).
[3] Global Biofuel Mandates, retrieved on 26 April, 2014 http://globalrfa.org/biofuels-map/ .
[4] U.S.D.o. Energy, National Algal Biofuels Technology Roadmap, 2010. (http://www1.eere.energy.gov/bioenergy/).
[5] J. Benemann, B. Koopman, J. Weissman, D. Eisenberg, R. Goebel, Development of microalgae harvesting and high-rate pond technologies in California, in: G. Shelef, C.J. Soeder (Eds.), Algae Biomass: Production and Use, Elsevier/North-Holland Biomedical Press, Amsterdam, The Netherlands, 1980.
[6] C.M. Beal, C.H. Smith, M.E. Webber, R.S. Ruoff, R.E. Hebner, A framework to report the production of renewable diesel from algae, Bioenergy Res. 4 (2011) 36–60.
[7] ANL; NREL; PNNL. (June 2012). *Renewable Diesel from Algal Lipids: An Integrated Baseline for Cost Emissions, and Resource Potential from a Harmonized Model.* ANL/ESD/12-4; NREL/TP-5100-55431; PNNL-21437. Argonne, IL: Argonne National Laboratory; Golden, CO: National Renewable Energy Laboratory; Richland, WA: Pacific Northwest National Laboratory.
[8] M.S. Peters, K.D. Timmerhaus, Plant Design and Economics for Chemical Engineers, Third ed. McGraw-Hill Book Company, New York, NY, 1980.
[9] R. Davis, A. Aden, P.T. Pienkos, Techno-economic analysis of autotrophic microalgae for fuel production, Appl. Energy 88 (2011) 3524–3531.
[10] A. Sun, R. Davis, M. Starbuck, A. Ben-Amotz, R. Pate, P.T. Pienkos, Comparative cost analysis of algal oil production for biofuels, Energy 36 (2011) 5169–5179.
[11] A. Tabernero, E.M. Martin del Valle, M.A. Galan, Evaluating the industrial potential of biodiesel from a microalgae heterotrophic culture: scale-up and economics, Biochem. Eng. J. 63 (2012) 104–115.
[12] S.D. Rios, C.M. Torres, C. Torres, J. Salvado, J.M. Mateo-Sanz, L. Jimenez, Microalgae-based biodiesel: economic analysis of downstream process realistic scenarios, Bioresour. Technol. 136 (2013) 617–624.
[13] E.M. Grima, E.-H. Belarbi, F.G. Acien Fernandez, A. Robles Medina, Y. Chisti, Recovery of microalgal biomass and metabolites: process options and economics, Biotechnol. Adv. 20 (2003) 491–515.
[14] L. Brennan, P. Owende, Biofuels from microalgae—A review of technologies for production, processing, and extractions for biofuels and co-products, Renew. Sust. Energ. Rev. 14 (2010) 557–577.
[15] H.C. Greenwell, L.M.L. Laurens, R.J. Shields, R.W. Lovitt, K.J. Flynn, Placing microalgae on the biofuels priority list: a review of the technological challenges, J. R. Soc. Interface 7 (2010) 703–726.
[16] N. Uduman, Y. Qi, M.K. Danquah, G.M. Forde, A. Hoadley, Dewatering of microalgal cultures: a major bottleneck to algae-based fuels, J. Renew. Sustain. Energy 2 (2010).
[17] H.M. Amara, A.C. Guedes, F. Xavier Malcata, Advances and perspectives in using microalgae to produce biodiesel, Appl. Energy 88 (2011) 3402–3410.
[18] L. Christenson, R. Sims, Production and harvesting of microalgae for wastewater treatment, biofuels, and bioproducts, Biotechnol. Adv. 29 (2011) 686–702.

[19] D. Aitken, B. Antizar-Ladislao, Achieving a green solution: limitations and focus points for sustainable algal fuels, Energies 5 (2012) 1613–1647.
[20] J. Kim, G. Yoo, H. Lee, J. Lim, K. Kim, C.W. Kim, M.S. Park, J.-W. Yang, Methods of downstream processing for the production of biodiesel from microalgae, Biotechnol. Adv. 31 (2013) 862–876.
[21] J.J. Milledge, S. Heaven, A review of the harvesting of micro-algae for biofuel production, Rev. Environ. Sci. Biotechnol. 12 (2013) 165–178.
[22] I. Rawat, R. Ranjith Kumar, T. Mutanda, F. Bux, Biodiesel from microalgae: a critical review from laboratory to large scale production, Appl. Energy 103 (2013) 444–467.
[23] S.F. Sing, A. Isdepsky, M.A. Borowitzka, N.R. Moheimani, Production of biofuels from microalgae, Mitig. Adapt. Strateg. Glob. Chang. 18 (2013) 47–72.
[24] P.E. Wiley, J.E. Campbell, B. McKuin, Production of biodiesel and biogas from algae: a review of process train options, Water Environ. Res. 83 (2011) 326–338.
[25] B.S. Massey, Mechanics of Fluids, 4th ed. Van Nostrand Reinhold Co. Ltd., Berkshire, England, 1980.
[26] M. Rickman, J. Pellegrino, R. Davis, Fouling phenomena during membrane filtration of microalgae, J. Membr. Sci. 423–424 (2012) 33–42.
[27] W. Liu, N. Canfield, Development of thin porous metal sheet as micro-filtration membrane and inorganic membrane support, J. Membr. Sci. 409–410 (2012) 113–126.
[28] M.R. Bilad, D. Vandamme, I. Foubert, K. Muylaert, I.F.J. Vankelecom, Harvesting microalgal biomass using submerged microfiltration membranes, Bioresour. Technol. 111 (2012) 343–352.
[29] T. De Baerdemaeker, B. Lemmens, C. Dotremont, J. Fret, L. Roef, K. Goiris, L. Diels, Benchmark study on algae harvesting with backwashable submerged flat panel membranes, Bioresour. Technol. 129 (2013) 582–591.
[30] X. Zhang, Q. Hu, M. Sommerfield, E. Puruhito, Y. Chen, Harvesting algal biomass for biofuels using ultrafiltration membranes, Bioresour. Technol. 101 (2010) 5297–5304.
[31] B. Petrusevski, G. Bolier, A.N. Van Breemen, G.J. Alaerts, Tangential flow filtration: a method to concentrate freshwater algae, Water Res. 29 (1995) 1419–1424.
[32] M.K. Danquah, L. Ang, N. Uduman, N. Moheimani, G.M. Forde, Dewatering of microalgal culture for biodiesel production: exploring polymer flocculation and tangential flow filtration, J. Chem. Technol. Biotechnol. 84 (2009) 1078–1083.
[33] R. Bhave, T. Kuritz, L. Powell, D. Adcock, Membrane-based energy efficient dewatering of microalgae in biofuels production and recovery of value added co-products, Environ. Sci. Technol. 46 (2012) 5599–5606.
[34] S.D. Rios, J. Salvado, X. Farriol, C. Torras, Antifouling microfiltration strategies to harvest microalgae for biofuel, Bioresour. Technol. 119 (2012) 406–418.
[35] S.S. Adham, J.G. Jacangelo, J.-M. Laine, Characteristics and costs of MF and UF plants, J. Am. Water Works Assoc. 88 (1996) 22–31.
[36] C.S. Vickers, Cost of Microfiltration and Ultrafiltration Membrane Systems, Microfiltration and Ultrafiltration Membranes for Drinking Water: Manual of Water Supply Practices, American Water Works Association, 2005.
[37] U.S. EPA, Technologies and Costs Document for the Final Long Term 2 Enhanced Surface Water Treatment Rule and Final Stage 2 Disinfectants and Disinfection Byproducts Rule, EPA 815-R-05-013, 2005.
[38] Chemical Engineering, Plant Cost Index, retrieved on 11/21/2013, http://www.che.com/pci/ .
[39] A.B. Aragon, R.B. Padilla, J.A. Fiestas Ros de Ursinos, Experimental study of the recovery of algae cultured in effluents from the anaerobic biological treatment of urban wastewaters, Resour. Conserv. Recycl. 6 (1992) 293–302.
[40] E. Poelman, N. De Pauw, B. Jeurissen, Potential of electrolytic flocculation for recovery of micro-algae, Resour. Conserv. Recycl. 19 (1997) 1–10.
[41] C.G. Alfafara, K. Nakano, N. Nomura, T. Igarashi, M. Matsumura, Operating and scale-up factors of the electrolytic removal of algae from eutrophied lakewater, J. Chem. Technol. Biotechnol. 77 (2002) 871–876.
[42] D. Vandamme, S.C.V. Pontes, K. Goiris, I. Foubert, L.J.J. Pinoy, K. Muylaert, Evaluation of electro-coagulation–flocculation for harvesting marine and freshwater microalgae, Biotechnol. Bioeng. 108 (2011) 2320–2329.
[43] J. Kim, B.-G. Ryu, B.-G. Kim, J.-I. Han, J.-W. Yang, Continuous microalgae recovery using electrolysis with polarity exchange, Bioresour. Technol. 111 (2012) 268–275.
[44] A.K. Lee, D.M. Lewis, P.J. Ashman, Harvesting of marine microalgae by electroflocculation: the energetics, plant design, and economics, Appl. Energy 108 (2013) 45–53.
[45] G. Mouedhen, M. Feki, M. De Petris Wery, H.F. Ayedi, Behavior of aluminum electrodes in electrocoagulation processes, J. Hazard. Mater. 150 (2008) 124–135.
[46] J.C. Donini, J. Kan, J. Szynkarczuk, T.A. Hassan, K.L. Kar, The operating cost of electrocoagulation, Can. J. Chem. Eng. 72 (1994) 1007–1012.
[47] S.J. Lee, M.-H. Jang, H.-S. Kim, B.-D. Yoon, H.-M. Oh, Variation of microcystin content of *Microcystis aeruginosa* relative to medium N:P ratio and growth stage, J. Appl. Microbiol. 89 (2000) 323–329.
[48] Historical statistics for mineral and material commodities in the United States (2013 version), retrieved on April 28, 2014, http://minerals.usgs.gov/minerals/pubs/historical-statistics/ .
[49] C.M. Ambler, The evaluation of centrifuge performance, Chem. Eng. Prog. 48 (1952) 150–158.
[50] C.M. Ambler, The theory of scaling up laboratory data for the sedimentation type centrifuge, J. Biochem. Microbiol. Technol. Eng. 1 (1959) 185–205.
[51] J. Happel, H.B. Brenner, Low Reynolds Number Hydrodynamics, Prentice Hall, Inc., Englewood Cliffs, NJ, 1965.
[52] C.S. Reynolds, Mechanisms of Suspension, The Ecology of Freshwater Phytoplankton, Cambridge University Press, Cambridge, UK, 1984.
[53] N.M. Burns, F. Rosa, In situ measurement of the settling velocity of organic carbon particles and 10 species of phytoplankton, Limnol. Oceanogr. 25 (1980) 855–864.
[54] S.K. Choi, J.Y. Lee, D.Y. Kwon, K.J. Cho, Settling characteristics of problem algae in the water treatment process, Water Sci. Technol. 53 (2006) 113–119.
[55] B.T. Smith, R.H. Davis, Particle concentration using inclined sedimentation via sludge accumulation and removal for algae harvesting, Chem. Eng. Sci. 91 (2013) 79–85.
[56] C.M. Ambler, J.C. Smith, Centrifuges, in: R.H. Perry, C.H. Chilton (Eds.), Chemical Engineers' Handbook, Section, 19, McGraw-Hill Book Company, New York, NY, 1973, pp. 87–101.
[57] M. Groschl, Ultrasonic separation of suspended particles - Part I: fundamentals, Acta Acust. 84 (1998) 432–447.
[58] S.M. Woodside, B.D. Bowen, J.M. Piret, Measurement of ultrasonic forces for particle–liquid separations, AIChE J. 43 (1997) 1727–1736.
[59] M.A. Weiser, R.E. Apfel, E.A. Neppiras, Interparticle forces on red cells in a standing wave field, Acustica 56 (1984) 114–119.
[60] K. Yosioka, Y. Kawasima, Acoustic radiation pressure on a compressible sphere, Acustica 5 (1955) 167–173.
[61] H. Nowotny, E. Benes, General one-dimensional treatment of the layered piezoelectric resonator with two electrodes, J. Acoust. Soc. Am. 82 (1987) 513–521.
[62] Metcalf & Eddy, Wastewater Engineering: Treatment, Disposal, and Reuse, Third ed McGraw-Hill, Inc, New York, NY, 1991.
[63] R. Bosma, W.A. Spronsen, J. Tramper, R.H. Wijffels, Ultrasound, a new separation technique to harvest microalgae, J. Appl. Phycol. 15 (2003) 143–153.
[64] M. Groschl, Ultrasonic separation of suspended particles - Part II: design and operation of separation devices, Acustica 84 (1998) 632–642.
[65] C.I. Nindo, J. Tang, Refractance window dehydration technology: a novel contact drying method, Dry. Technol. 25 (2007) 37–48.
[66] M. Cooney, G. Young, N. Nagle, Extraction of bio-oils from microalgae, Sep. Purif. Rev. 38 (2009) 291–326.
[67] W.T. Coakley, A.J. Bater, D. Lloyd, Disruption of micro-organisms, in: A.H. Rose, D. W. Tempest (Eds.), Advances in Microbial Physiology, Academic Press, New York, NY, 1977.
[68] Y. Chisti, M. Moo-Young, Disruption of microbial cells for intracellular products, Enzym. Microb. Technol. 8 (1986) 194–207.
[69] A.P.J. Middelberg, Process-scale disruption of microorganisms, Biotechnol. Adv. 13 (1995) 491–551.
[70] G.J. Gil-Chavez, J.A. Villa, J.F. Ayala-Zavala, J.B. Heredia, D. Sepulveda, E.M. Yahia, G. A. Gonzalez-Aguilar, Technologies for extraction and production of bioactive compounds to be used as nutraceuticals and food ingredients: an overview, Compr. Rev. Food Sci. Food Saf. 12 (2013) 5–23.
[71] K. de Boer, N.R. Moheimani, M.A. Borowitzka, P.A. Bahri, Extraction and conversion pathways for microalgae to biodiesel: a review focused on energy consumption, J. Appl. Phycol. 24 (2012) 1681–1698.
[72] P. Mercer, R.E. Armenta, Developments in oil extraction from microalgae, Eur. J. Lipid Sci. Technol. 113 (2011) 539–547.
[73] R. Halim, M.K. Danquah, P.A. Webley, Extraction of oil from microalgae for biodiesel production: a review, Biotechnol. Adv. 30 (2012) 709–732.
[74] A. Wileman, A. Ozkan, H. Berberoglu, Rheological properties of algae slurries for minimizing harvesting energy requirements in biofuel production, Bioresour. Technol. 104 (2012) 432–439.
[75] H. Desmorieux, N. Decaen, Convective drying of spirulina in thin layer, J. Food Eng. 66 (2005) 497–503.
[76] R.A. Lemus, M. Perez, A. Andres, T. Roco, C.M. Tello, A. Vega, Kinetic study of dehydration and desorption isotherms of red alga *Gracilaria*, Food Sci. Technol. 41 (2008) 1592.
[77] M.C. Hnini, M. Benchanaa, M.E. Hammioui, Study of the interaction between water and *Gelidium sesquipedale* (Rhodophyta). Part I: thermodynamic aspect of the sorption equilibrium, Journal of the Taiwan Institute of Chemical Engineers 44 (2013) 195–801.
[78] T. Lewis, P.D. Nichols, T.A. McMeekin, Evaluation of extraction methods for recovery of fatty acids from lipid-producing microheterotrophs, J. Microbiol. Methods 43 (2000) 107–116.
[79] F. Smedes, T.K. Askland, Revisiting the development of the Bligh and Dyer total lipid determination method, Mar. Pollut. Bull. 38 (1999) 193–201.
[80] E.G. Bligh, W.J. Dyer, A rapid method of total lipid extractin and purification, Can. J. Biochem. Physiol. 37 (1959) 911–917.
[81] H. Kanda, P. Li, Simple extraction method of green crude from natural blue-green microalgae by dimethyl ether, Fuel 90 (2011) 1264–1266.
[82] H. Kanda, P. Li, T. Ikehara, M. Yasumoto-Hirose, Lipids extracted from several species of natural blue-green microalgae by dimethyl ether: extraction yield and properties, Fuel 95 (2012) 88–92.
[83] H. Kanda, P. Li, T. Yoshimura, S. Okada, Wet extraction of hydrocarbons from *Botryococcus braunii* by dimethyl ether as compared with dry extraction by hexane, Fuel 105 (2013) 535–539.
[84] L. Yao, J.A. Gerde, T. Wang, Oil extraction from microalga *Nannochloropsis* sp. with isopropyl alcohol, J. Am. Oil Chem. Soc. 89 (2012) 2279–2287.
[85] C.D. Tanzi, M. Abert-Vian, C. Ginies, M. Elmaataoui, F. Chemat, Terpenes as green solvents for extraction of oil from microalgae, Molecules 17 (2012) 8196–8205.
[86] C.D. Tanzi, M. Abert-Vian, F. Chemat, New procedure for extraction of algal lipids from wet biomass: a green clean and scalable process, Bioresour. Technol. 134 (2013) 271–275.
[87] N. Samarasinghe, S. Fernando, R. Lacey, W.B. Faulkner, Algal cell rupture using high pressure homogenization as a prelude to oil extraction, Renew. Energy 48 (2012) 300–308.
[88] R. Halim, T.W.T. Rupasinghe, D.L. Tull, P.A. Webley, Mechanical cell disruption for lipid extraction from microalgal biomass, Bioresour. Technol. 140 (2013) 53–63.

[89] E.M. Spiden, B.H.J. Yap, D.R.A. Hill, S.E. Kentish, P.J. Scales, G.J.O. Martin, Quantitative evaluation of the ease of rupture of industrially promising microalgae by high pressure homogenization, Bioresour. Technol. 140 (2013) 165–171.
[90] G. Hedenskog, L. Enebo, J. Vendlova, B. Prokes, Investigation of some methods for increasing the digestibility in vitro of microalgae, Biotechnol. Bioeng. 11 (1969) 37–51.
[91] J. Doucha, K. Livansky, Influence of processing parameters on disintegration of *Chlorella* cells in various types of homogenizers, Appl. Microbiol. Biotechnol. 81 (2008) 431–440.
[92] J.-Y. Lee, C. Yoo, S.-Y. Jun, C.-Y. Ahn, H.-M. Oh, Comparison of several methods for effective lipid extraction from microalgae, Bioresour. Technol. 101 (2010) S75–S77.
[93] F. Adam, M. Abert-Vian, G. Peltier, F. Chemat, "Solvent-free" ultrasound-assisted extraction of lipids from fresh microalgae cells: a green, clean, and scalable process, Bioresour. Technol. 114 (2012) 457–465.
[94] J.A. Gerde, M. Montalbo-Lomboy, L. Yao, D. Grewell, T. Wang, Evaluation of microalgae cell disruption by ultrasonic treatment, Bioresour. Technol. 125 (2012) 175–181.
[95] S. Dey, V.K. Rathod, Ultrasound assisted extraction of b-carotene from *Spirulina platensis*, Ultrason. Sonochem. 20 (2013) 271–277.
[96] T.A. Bigelow, J. Xu, D.J. Stessman, L. Yao, M.H. Spalding, T. Wang, Lysis of *Chlamydomonas reinhardtii* by high-intensity focused ultrasound as a function of time of exposure, Ultrason. Sonochem. 21 (2014) 1258–1264.
[97] J. Sheng, R. Vannela, B.E. Rittmann, Evaluation of cell-disruption effects of pulsed-electric-field treatment of Synchocystis PCC 6803, Environ. Sci. Technol. 45 (2011) 3795–3802.
[98] J. Sheng, R. Vannela, B.E. Rittmann, Disruption of Synechocystis PCC 6803 for lipid extraction, Water Sci. Technol. 65 (2012) 567–573.
[99] A.E. Sowers, Overview of electroporation and electrofusion, in: D.C. Chang, B.M. Chassy, J.A. Saunders, A.E. Sowers (Eds.), Guide to Electroporation and Electrofusion, Academic Press, Inc., San Diego, CA, 1992.
[100] T. Geng, C. Lu, Microfluidic electroporation for cellular analysis and delivery, Lab Chip 13 (2013) 3803–3821.
[101] A.K. Lee, D.M. Lewis, P.J. Ashman, Disruption of microalgal cells for the extraction of lipids for biofuels: process and specific energy requirements, Biomass Bioenergy 46 (2012) 89–101.
[102] A.K. Lee, D.M. Lewis, P.J. Ashman, Force and energy requirement for microalgal cell disruption: an atomic force microscope evaluation, Bioresour. Technol. 128 (2013) 199–206.
[103] K. Takisawa, K. Kanemoto, T. Miyazaki, Y. Kitamura, Hydrolysis for direct esterification of lipids from wet microalgae, Bioresour. Technol. 144 (2013) 38–43.
[104] U.S. Department of Energy, Hydrogen Data Resource Center Lower and Higher Heating Values, retrieved on May 4, 2014, http://hydrogen.pnl.gov/cocoon/morf/projects/hydrogen/datasheets/lower_and_higher_heating_values.xls
[105] A.M. Illman, A.H. Scragg, S.W. Shales, Increase in *Chlorella* strains calorific values when grown in low nitrogen medium, Enzym. Microb. Technol. 27 (2000) 631–635.
[106] Y. Chisti, Biodiesel from microalgae, Biotechnol. Adv. 25 (2007) 294–306.
[107] P.H. Pfromm, V. Amanor-Boadu, R. Nelson, Sustainability of algae derived biodiesel: a mass balance approach, Bioresour. Technol. 102 (2011) 1185–1193.
[108] C.M. Beal, R.E. Hebner, M.E. Webber, Thermodynamic analysis of algal biocrude production, Energy 44 (2012) 925–943.
[109] U.S. Energy Information Administration, Average annual industrial retail price for electricity from 2003 to 2012, retrieved on 11/20/2013, http://www.eia.gov/electricity/data.cfm .
[110] A.J. Dassey, C.S. Teegala, Harvesting economics and strategies using centrifugation for cost effective separation of microalgae cells for biodiesel applications, Bioresour. Technol. 128 (2013) 241–245.
[111] M.J. Griffiths, S.T.L. Harrison, Lipid productivity as a key characteristic for choosing algal species for biodiesel production, J. Appl. Phycol. 21 (2009) 493–507.
[112] G. Petkov, A. Ivanova, I. Iliev, I. Vaseva, A critical look at the microalgae biodiesel, Eur. J. Lipid Sci. Technol. 114 (2012) 103–111.
[113] P. Kumar, M.R. Suseela, K. Toppo, Physico-chemical characterization of algal oil: a potential biofuel, Asian J. Exp. Biol. Sci. 2 (2011) 493–497.
[114] L. Rodolfi, G. Chini Zittelli, N. Bassi, G. Padovani, N. Biondi, G. Bonini, M.R. Tredici, Microalgae for oil: strain selection, induction of lipid synthesis and outdoor mass cultivation in a low-cost photobioreactor, Biotechnol. Bioeng. 102 (2009) 100–112.
[115] A.H. Scragg, A.M. Illman, A. Carden, S.W. Shales, Growth of microalgae with increased calorific values in a tubular bioreactor, Biomass Bioenergy 23 (2002) 67–73.
[116] K.M. Weyer, D.R. Bush, A. Darzins, B.D. Wilson, Theoretical maximum algal oil production, Bioenergy Res. 3 (2010) 204–213.
[117] P.E. Zemke, B.D. Wood, D.J. Dye, Considerations for the maximum production rates of triacylglycerol from microalgae, Biomass Bioenergy 34 (2010) 145–151.
[118] X. Miao, Q. Wu, C. Yang, Fast pyrolysis of microalgae to produce renewable fuels, J. Anal. Appl. Pyrolysis 71 (2004) 855–863.
[119] N. Uduman, V. Bourniquel, M.K. Danquah, A.F.A. Hoadley, A parametric study of electrocoagulation as a recovery process of marine microalgae for biodiesel production, Chem. Eng. J. 174 (2011) 249–257.
[120] T.N. Pashovkin, D.G. Sadikova, Cell exfoliation, separation, and concentration in the field of a standing ultrasonic wave, Acoust. Phys. 55 (2009) 584–593.
[121] J. Kim, J.W. Choi, D. Kang, Laboratory experiment to measure 5-MHz volume backscattering strengths from *red-tide* causing microalgae *Chattonella antiqua*, Ocean Sci. J. 47 (2012) 173–179.
[122] C.F. Greenlaw, R.K. Johnson, Physical and acoustical properties of zooplankton, J. Acoust. Soc. Am. 72 (1982) 1706–1710.
[123] R.C. Weast, CRC Handbook of Chemistry and Physics, CRC Press, Inc., Boca Raton, FL, 1983.
[124] C.-T. Chen, F.J. Millero, Speed of sound in seawater at high pressures, J. Acoust. Soc. Am. 62 (1977) 1129–1135.
[125] K.G. Foote, Speed of sound in *Euphausia superba*, J. Acoust. Soc. Am. 87 (1990) 1405–1408.
[126] C.C. Clay, H. Medwin, Acoustical Oceanography: Principles and Applications, John Wiley & Sons, Inc., 1977
[127] R.W. Eppley, R.W. Holmes, J.D.H. Strickland, Sinking rates of marine phytoplankton measured with a fluorometer, J. Exp. Mar. Biol. Ecol. 1 (1967) 199–208.
[128] S. Kashyap, A. Sundararajan, L.-K. Ju, Flotation characteristics of cyanobacterium *Anabaena flos-aquae* for gas vesicle production, Biotechnol. Bioeng. 60 (1998) 636–641.
[129] A.S. Foust, L.A. Wenzel, C.W. Clump, L. Maus, L.B. Anderson, Principles of Unit Operations, Second Edition John Wiley & Sons, New York, NY, 1980.
[130] B.G. Morris, Applications and selection of centrifuges, Br. Chem. Eng. 11 (1966) 347–351.
[131] L. Svarovsky, Separation by centrifugal sedimentation, in: L. Svarovsky (Ed.), Solid–Liquid Separation, 2001, pp. 246–280.
[132] M. Boychyn, S.S.S. Yim, M. Bulmer, J. More, D.G. Bracewell, M. Hoare, Performance prediction of industrial centrifuges using scale-down models, Bioprocess Biosyst. Eng. 26 (2004) 385–391.